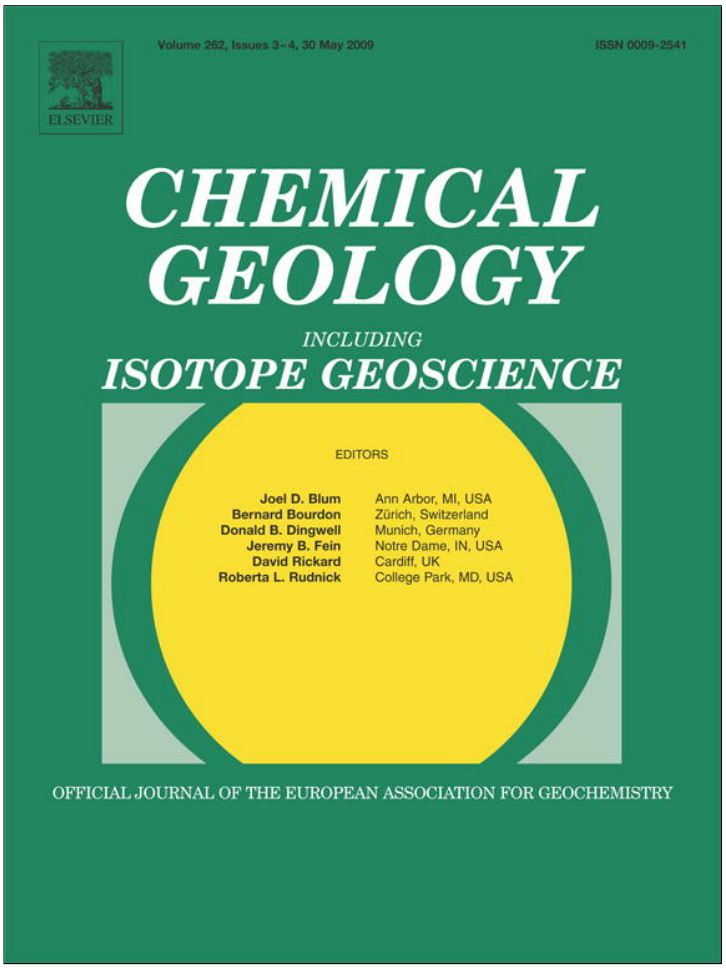

Chemical Geology 262 (2009) 202–216

Contents lists available at ScienceDirect

Chemical Geology

journal homepage: www.elsevier.com/locate/chemgeo

Late Miocene sea surface salinity variability and paleoclimate conditions in the Eastern Mediterranean inferred from coral aragonite $\delta^{18}O$

R. Mertz-Kraus [a,b,*], T.C. Brachert [a,c], M. Reuter [d], S.J.G. Galer [b], C. Fassoulas [e], G. Iliopoulos [e]

[a] Johannes Gutenberg-Universität, Institut für Geowissenschaften, Becher-Weg 21, 55099 Mainz, Germany
[b] Max-Planck-Institut für Chemie, Postfach 3060, 55020 Mainz, Germany
[c] Universität Leipzig, Institut für Geophysik und Geologie, Talstr. 35, 04103 Leipzig, Germany
[d] Karl-Franzens-Universität Graz, Institut für Erdwissenschaften, Bereich Geologie und Paläontologie, Heinrichstr. 26, 8010 Graz, Austria
[e] Natural History Museum, University of Crete, 71409 Iraklion, Greece

ARTICLE INFO

Article history:
Received 7 June 2008
Received in revised form 25 December 2008
Accepted 17 January 2009

Editor: D. Rickard

Keywords:
Paleoclimate
Coral $\delta_{18}O$
Sea surface salinity
Sea surface temperature
Late Miocene
Eastern Mediterranean

ABSTRACT

Coral skeletons are archives of chemical proxies which enable paleoenvironmental reconstructions to be made at subannual resolution. Stable oxygen isotope ($\delta^{18}O$) ratios of these archives reflect sea surface temperature (SST) as well as the $\delta^{18}O$ composition of ambient seawater. The $\delta^{18}O_{seawater}$ composition is not only controlled by global ice build-up, but river discharge and the hydrological balance of evaporation and precipitation, all influencing sea surface salinity (SSS), also play an important role in marginal seas. New subannually resolved coral $\delta^{18}O$ data were measured and evaluated together with published data from reef coral communities of Late Miocene age from Crete (Eastern Mediterranean). This time-window is of particular importance for the paleoceanographic evolution of the Mediterranean Sea, because it covers the successive closure of the marine gateways connecting the Mediterranean with the Atlantic Ocean, which culminated in the onset of the Messinian salinity crisis (MSC) at 5.96 Ma. Corals were recovered from eight time-slices dated by $^{87}Sr/^{86}Sr$ chronostratigraphy and cover a time-window from ~10 to ~7 Ma to monitor pre-MSC environmental changes. The oxygen isotope composition of the reef corals *Porites* and *Tarbellastraea* document significant changes in mean annual $\delta^{18}O$ as well as in mean $\delta^{18}O$ seasonality during the Late Miocene. Tortonian and Messinian coral mean annual $\delta^{18}O$ values differ by up to 1.72‰ and exhibit substantial variability. Since SSTs can be considered rather constant over the Late Miocene according to lithological, paleobotanical and geochemical evidence, the mean annual $\delta^{18}O$ variations in the corals appear to result from changing SSS during the Late Miocene prior to the MSC. This result is in contrast to earlier concepts that, despite increasing isolation of the Mediterranean basin starting at about 9 Ma ago, SSS did not change until only 300 kyr prior to the deposition of the first MSC evaporites. Mean seasonal $\delta^{18}O$ amplitudes are lower by 0.4‰ in the Messinian compared to those of the Tortonian corals, which may be due to enhanced summer evaporation. Spectral analyses of Tortonian and Messinian coral $\delta^{18}O$ records indicate significant interannual variability with periods of 2–3 and 4–5 years. Such variability is similar to that found in modern records. In the modern case, the Iceland Low and Azores High pressure centers influence climate in the Circum-Mediterranean region. Combined with evidence from other studies, the coral records of this study suggest that a similar pressure field system was already in existence in the early Late Miocene.

1. Introduction

The Late Miocene sedimentary record of the Mediterranean region heralds one of the most profound geological events of the Cenozoic: increasing Mediterranean restriction, partial desiccation and marine refilling during the Messinian salinity crisis (MSC) ~6 Ma ago (Hsü et al., 1977). Although many problems regarding "the chronology, causes and progression of the MSC" (Krijgsman et al., 1999) remain, a consistent pattern has started to emerge (Rouchy and Caruso, 2006). According to Sr isotope data from foraminifera, the Atlantic–Mediterranean water mass exchange started to be increasingly severed about 9 Ma ago, 3 Myr earlier than accumulation of the first evaporites of the MSC. However, salinity is usually believed to have remained essentially constant and marine in the Mediterranean basin during this pre-evaporite period because evaporation was balanced by deep brine outflow and freshwater discharge and/or precipitation (Flecker and Ellam, 1999, 2006). The geological expression of this situation is an omnipresent suite of conspicuous marl–sapropel cycles because freshwater input was not constant but strongly pulsed at

* Corresponding author. Johannes Gutenberg-Universität, Institut für Geowissenschaften, Becher-Weg 21, 55099 Mainz, Germany. Tel.: +49 6131 3923247; fax: +49 6131 3924768.
E-mail address: mertzre@uni-mainz.de (R. Mertz-Kraus).

0009-2541/$ – see front matter © 2009 Elsevier B.V. All rights reserved.
doi:10.1016/j.chemgeo.2009.01.010

precessional time-scales (Hilgen et al., 1995; Schenau et al., 1999). Associated salinity and/or water temperature changes are well documented in various stable isotope and micropaleontological data sets from the Circum-Mediterranean region. Typically, $\delta^{18}O$ values of Late Miocene microfossils from different sedimentary sections within the Mediterranean region show enhanced variations in the course of the Late Miocene compared to the Late Miocene open ocean (Santarelli et al., 1998; Kouwenhoven et al., 1999; Perez-Folgado et al., 2003; Sierro et al., 2003). As a consequence of continual restriction, hinterland climate (including remote precipitation of the African monsoon) played an increasingly significant role in Mediterranean hydrography and as a pacemaker of the geological record (Tzedakis, 2007; Rohling et al., 2008). However, on the basis of vegetational data, it is generally thought that modern Mediterranean climate with hot, dry summers and mild, wet winters did not develop before 3.6 Ma (Suc, 1984; Suc and Popescu, 2005) whereas winter precipitation has been reinforced during Pleistocene episodes of sapropel formation (Wijmstra et al., 1990). Subannually resolved stable isotope data from reef corals (*Porites*) of Late Miocene age and climate model results, however, suggest the modern climatic system appeared earlier in the course of the Tertiary or before (Brachert et al., 2006a).

Despite detailed knowledge of pelagic and terrestrial high-frequency ecosystem change in response to climatic fluctuations and Mediterranean restriction, very little is known about its effects on shallow water benthic ecosystems. Previous studies focused on sedimentary facies analysis and sea-level signatures in reefs and carbonate platforms (Pomar, 1991; Esteban, 1996). For the Western Mediterranean region, sea-level change was found to be in phase with sea surface temperatures (SSTs) causing rhythmic reef demise and turnover in carbonate-producing biotic associations (Martín and Braga, 1994; Brachert et al., 1996). This fits more recent findings of pronounced glacial control on sea-level fluctuations during the Neogene (Billups and Schrag, 2003; Westerhold et al., 2005; Sánchez-Almazo et al., 2007) and stable isotope data, therefore, represent excellent proxy sets of Neogene sea level (Miller et al., 2005). In the Eastern Mediterranean region, cold Atlantic spells have not been clearly documented in Late Miocene SSTs (Kroeger et al., 2006), however, pulsed freshwater influx and sediment discharge, possibly responding to astronomical forcing, have been shown to be an important factor in controlling coral reef distribution during the Tortonian (Reuter and Brachert, 2007). A recent account of Mediterranean reef distribution during the Late Miocene is given by Brachert et al. (2006b). Usually, geochemical proxy records of the Neogene based on deep sea sedimentary successions resolve thousands of years and fail to reveal climate variability on interannual and seasonal timescales.

In this paper we show how geochemical coral data can be of particular significance to Neogene paleoclimatology. Usually, massive reef corals grow to large size in tropical–subtropical shallow-water environments and are especially sensitive to sea level, SST and sea surface salinity (SSS); however, aragonite saturation and nutrient concentrations are also important for coral growth (Kleypas et al., 1999). The massive skeletons, composed of $CaCO_3$ (aragonite), exhibit annual incremental growth and, therefore, represent excellent time-calibrated paleoenvironment archives (Druffel, 1997). Time-series of geochemical proxy data from the aragonite skeletons are extremely useful for describing environmental variability on subannual to decadal time scales for both, instrumental and pre-instrumental time periods (e.g., Druffel, 1997). Stable oxygen isotope ratios ($\delta^{18}O$) represent the most widely used coral geochemical proxy. However, its use as a paleothermometer is limited, because the $\delta^{18}O$ signal represents both SST and SSS, and ambient seawater $\delta^{18}O$ may vary in time and space as a result of local evaporation/precipitation and patterns of river discharge (Weber and Woodhead, 1972). SST calibrations from $\delta^{18}O$, therefore, require additional, independent geochemical proxy data (i.e. Sr/Ca) (Gagan et al., 2000). For geological time, however, such SST reconstructions remain problematic because of glacial changes in $\delta^{18}O$ of global sea water and secular variations in trace element ratios (Zachos et al., 2001; Lear et al., 2003). In order to overcome the problem of seawater effects on the $\delta^{18}O$ thermometer and other geochemical proxy data during the late Neogene, the statistically significant relationship between SST and annual extension or growth rate for certain reef corals (Lough and Barnes, 2000; Slowey and Crowley, 1995) can be applied (Brachert et al., 2006b).

Coral skeletons (*Porites*, *Tarbellastraea*) of Late Miocene age (Tortonian and Messinian) from the island of Crete (Eastern Mediterranean) were recovered from two areas representing eight time-slices covering the period from ~10 to ~7 Ma. The ~3 Myr-period covered by our sampling falls in the time of increasing restriction of the Mediterranean modulated by climatic changes on subannual to geological time scales. We compare our new data to published coral stable isotope time-series (Brachert et al., 2006a; Mertz-Kraus et al., 2008) in terms of average $\delta^{18}O$ composition and seasonal $\delta^{18}O$ variability in order to separate long-term effects of global sea level from Eastern Mediterranean evaporation/precipitation systems and freshwater discharge or salinity and seasonal SST changes. Our observations substantially complement views about the hydrological balance or freshwater discharge with climatic precession and seasonal distribution of precipitation/evaporation and can therefore help in completing our picture of Neogene Mediterranean climate dynamics and hydrography.

2. Geological context

Basins of Neogene age are scattered over the island of Crete and were formed following extensional geodynamic processes in the Aegean region during the Middle Miocene (Fassoulas, 2001; Meulenkamp

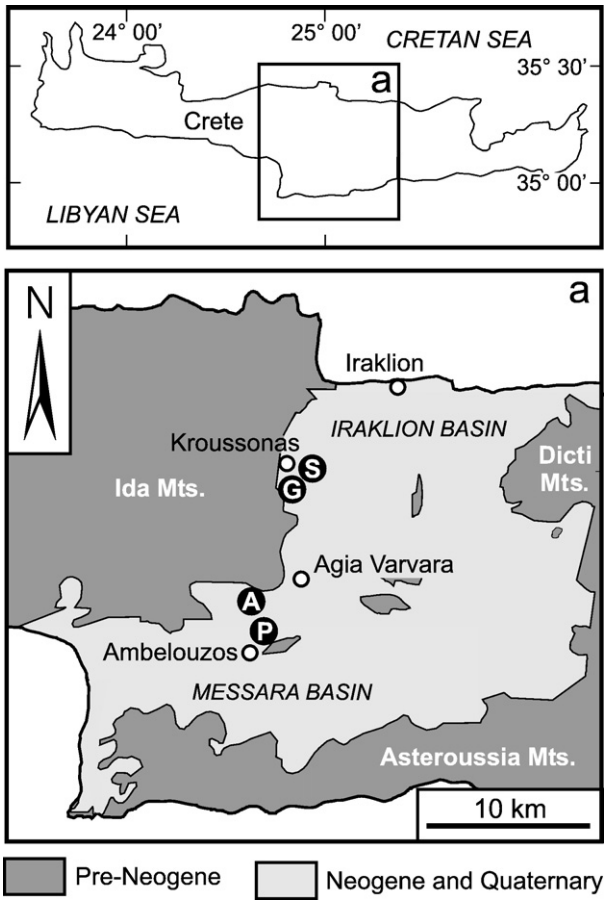

Fig. 1. Simplified geological map of Central Crete, Greece. (P) Psalidha, Tortonian, and (A) Apomarma, Early Messinian, Messara Basin; (G) Gorgolaini Monastery and (S) Sarhos, Early Messinian, western margin of Iraklion Basin.

and Sissingh, 2003). In this study, we focus on material sampled from Miocene sediments of the Iraklion and Messara Basins in Central Crete (Fig. 1). These sediments can be subdivided into two stratigraphic units: (1) the Ambelouzos Formation of Serravallian to Tortonian age, and (2) the Varvara Formation of Late Tortonian to Early Messinian age (Meulenkamp et al., 1979; ten Veen and Postma, 1999). The Ambelouzos Formation consists of clastic sediments, which have been attributed to brackish-lagoonal, marginally marine and open marine depositional environments where the climate was humid. Coral constructions representing both, biostromes and bioherms, are associated with coarse-grained delta deposits and marine clastics (Faranda et al., 2007; Reuter and Brachert, 2007). Sediments of the Varvara Formation overlay those of the Ambelouzos Formation, and comprise shallow marine limestones with reef corals (Pirgos Member), as well as deeper marine marls, with intercalated calciturbidites and debris flow deposits, and evaporites. The change from shallow marine clastics to carbonates, and finally evaporites reflects increasing sediment starvation of the basin with time. Such changes were most likely a

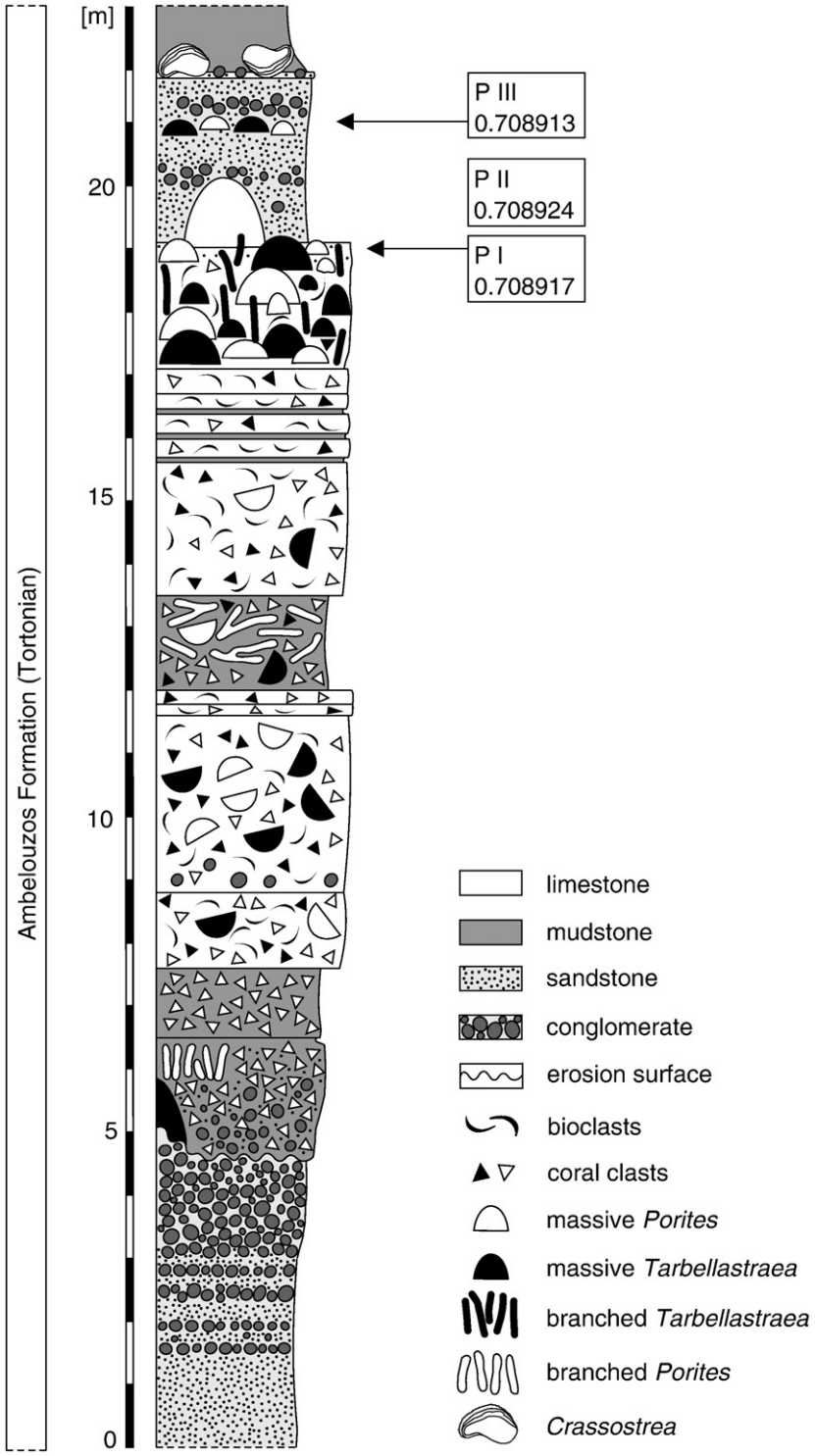

Fig. 2. Geological section at Psalidha with sampling sites P I, P II and P III (Tortonian) indicated, and respective mean $^{87}Sr/^{86}Sr$ values. P I is equivalent to CL 1.2 of Brachert et al. (2006b).

consequence of structural rejuvenations of the basin, long-term relative rise of sea level, and climatic aridification which took place during the course of the Late Miocene (Fassoulas, 2001; Reuter et al., 2006). In addition to long-term changes, Tortonian coral constructions reflect high-frequency variability of freshwater input and sediment discharge, possibly in response to climatic precession (Reuter and Brachert, 2007).

Stratal architectures and stacking patterns of seven unconformity-bound depositional units (or "Coral levels", CL of Brachert et al. (2006b)) were grouped into three larger-scale depositional sequences. They represent the backbone for the age model for Late Miocene shallow-water deposits of western Iraklion Basin in central Crete (Brachert et al., 2006b; Reuter et al., 2006). Units 1 to 3 represent the Early Tortonian sea-level cycle, Units 4 to 6 the Late Tortonian, and Unit 7 the Early Messinian eustatic cycles of Hardenbol et al. (1998), respectively. Since outcrops are isolated in most basins it is difficult to establish a stratigraphic framework on a larger geographical scale. Thus, it should be borne in mind that some corals described in this study cannot be placed univocally within the stratigraphy of the western Iraklion Basin.

3. Sampling sites

The coral samples are from two areas in central Crete which are at the northern margin of the Messara Basin and at the western margin of the Iraklion Basin, respectively (Fig. 1). In the northern Messara Basin, corals were samples at three sites near the abandoned town of Psalidha just north of the town of Ambelouzos (Fig. 1). Psalidha coral sites are within the lower segment of the Tortonian Ambelouzos Formation (Fig. 2) at the top of a coral build-up (thickness 15 m) and within the overlying unit of coarse clastics (thickness 3 m). The build-up exhibits prominent horizontal, parallel bedding resulting from the stacking of coral biostromes and bioclastic carbonates. *Porites* and *Tarbellastraea* are the dominant coral genera. A detailed sedimentological and paleoecological analysis is reported in Reuter and Brachert (2007).

Sampling site P I (E 24.96094°, N 35.08424°), identical with section B of Reuter and Brachert (2007), is located along the contact surface of the topmost biostrome with overlying sandstone and conglomerate. This site can be considered equivalent to the top of stratigraphic Unit 1 of the western Iraklion chronostratigraphic succession. Some of the corals along the contact are extremely large up to a height of ca. 1 m and dominated by massive *Porites* still in life position. This gives the stratigraphic surface a strongly undulating shape, with some of the corals being almost fully encased by cross-stratified sandstone or conglomerate. According to coral zonation patterns in Late Miocene reefs of the Mediterranean, water depth was <20 m. Site P III lies stratigraphically above and within the sandstone unit. It represents a small patch of massive, non framework-forming *Porites* (decimeter size) in life position (E 24.96038°, N 35.08498°). An oyster bed composed of *Crassostrea* sp. shells forms the top of the sandstone unit and indicates a very shallow, marginal marine environment (Kirby, 2001). It marks an abrupt transition into fine-grained sediments of the Ambelouzos Formation and final drowning of Psalidha reef site (Fig. 2). Site P II, congruent with section C of Reuter and Brachert (2007), is located in a nearby olive grove (linear distance ~550 m, E 24.96488°, N 35.08682), which is situated within the unit of coarse clastics on top of the build-up. Because of poor outcrop, corals were collected from soil, which obscures their exact stratigraphic position. However, the similarity in Sr isotope composition to that of corals from P I (Mertz-Kraus et al., 2008) suggests that P II lies stratigraphically between that of P I and P III, or perhaps is identical with P I. Combined lithostratigraphic and biostratigraphic data suggest an age of ~10 Ma for coral site P I (Brachert et al., 2006a; Faranda et al., 2007; Frydas et al., 2008) and an age of ~9 to 10 Ma for sites P II (Mertz-Kraus et al., 2007) based on $^{87}Sr/^{86}Sr$ chronostratigraphy.

The second set of sampling sites is located at the western margin of the Iraklion Basin, to the northwest of Gorgolaini Monastery (Fig. 1). The Gorgolaini section is 40 m thick and formed of sediments of Tortonian and Early Messinian age onlapping Pre-Neogene basement. Corals crop out in distinct stratigraphic levels and have been collected at sites G I, G II, G III, G IV and G V (Fig. 3). The lowermost sampling level G I (E 25.63861°, N 35.34819°) lies on top of a thick conglomerate and is composed of sandy marl containing coarse sand-granular lithoclasts and decimeter-sized corals in life position. Lithostratigraphically, this sampling level is located near the top of the Ambelouzos Formation and, in terms of sequence stratigraphy, is equivalent to Unit 4 (or CL 4) of Late Tortonian age (Brachert et al., 2006b). The section continues after ~8.5 m covered by vegetation and slope debris with a succession of bipartite cycles of laminated marl and homogeneous marl with thin intervening beds of calciturbidites and four thick beds of breccia interpreted as debrites (Fig. 3). These debrites contain lithoclasts of Pre-Neogene basement, Messinian vermetid limestone, and coral fragments, including almost complete specimens of *Porites* and *Tarbellastraea*. Coral size ranges from a few centimeters to several decimeters. Some of the corals have fully or partially retained their original aragonite mineralogy.

The upper part of the Gorgolaini section belongs to the lower Varvara Formation which has been assigned an Early Messinian biostratigraphic age (Meulenkamp et al., 1979). According to the sequence stratigraphic framework of the western Iraklion Basin, this section also corresponds to Unit 7 (CL 7), which correlates to the Early Messinian eustatic sea-level cycle (Hardenbol et al., 1998). The sampling sites G II, G IV and G V (E 24.9819°, N 35.20535°) of our study are equivalent to coral levels CL 7.1, CL 7.2 and CL 7.3 (Brachert et al., 2006b). A section of the Varvara Formation, with intercalated volcanic ash layers and base of slope deposits (turbidites) in Northern Messara Basin (Kastelli), was dated at 6.8 to 6.9 Ma (Hilgen et al., 1997; ten Veen and Postma, 1999), which is in agreement with an Early Messinian age for sites G II to G V. Distinct cycles of homogeneous marl and dark gray laminated marl within the Gorgolaini section might be equivalent to a conspicuous bipartite marl–sapropelite succession described from various locations on Crete, which reflect precession-driven climatic change (Krijgsman et al., 1995; Santarelli et al., 1998). On this basis, the top of the section at site G V might only be some hundreds of kyr younger than that of site G II.

4. Materials and methods

4.1. Sample preparation

In the field, only almost white-colored coral specimens with relatively low density were selected, because from personal sampling experience such specimens have proven to most likely represent corals having retained their primary aragonitic skeleton and porosity, respectively. In contrast, specimens not suitable for geochemical analyses have signs of neomorphosism, recrystallization and cementation, resulting in higher density.

In the laboratory, slabs of ~6 mm thickness were sliced out of each coral specimen parallel to the axis of maximum growth. After cleaning the slabs with a solution of hydrogen peroxide (<1%), contact radiographs were obtained using a Faxitron model 805 X-ray unit (3 mA, 45 kV, exposure time 6 to 9 min) and AGFA Structurix D4 FW Industrial X-ray film. X-ray diffraction (XRD), reflected light stereomicroscopic analysis and scanning electron microscopy (SEM) were performed on random samples in order to check for diagenetical alteration prior to preparation for radiogenic and stable isotope analysis. Based on the results of the outlined quality monitoring, only skeletal material with preservation of the original aragonite mineralogy was used further (Table 1) resulting in an about 20% rejection of specimens considered to be suitable during field sampling.

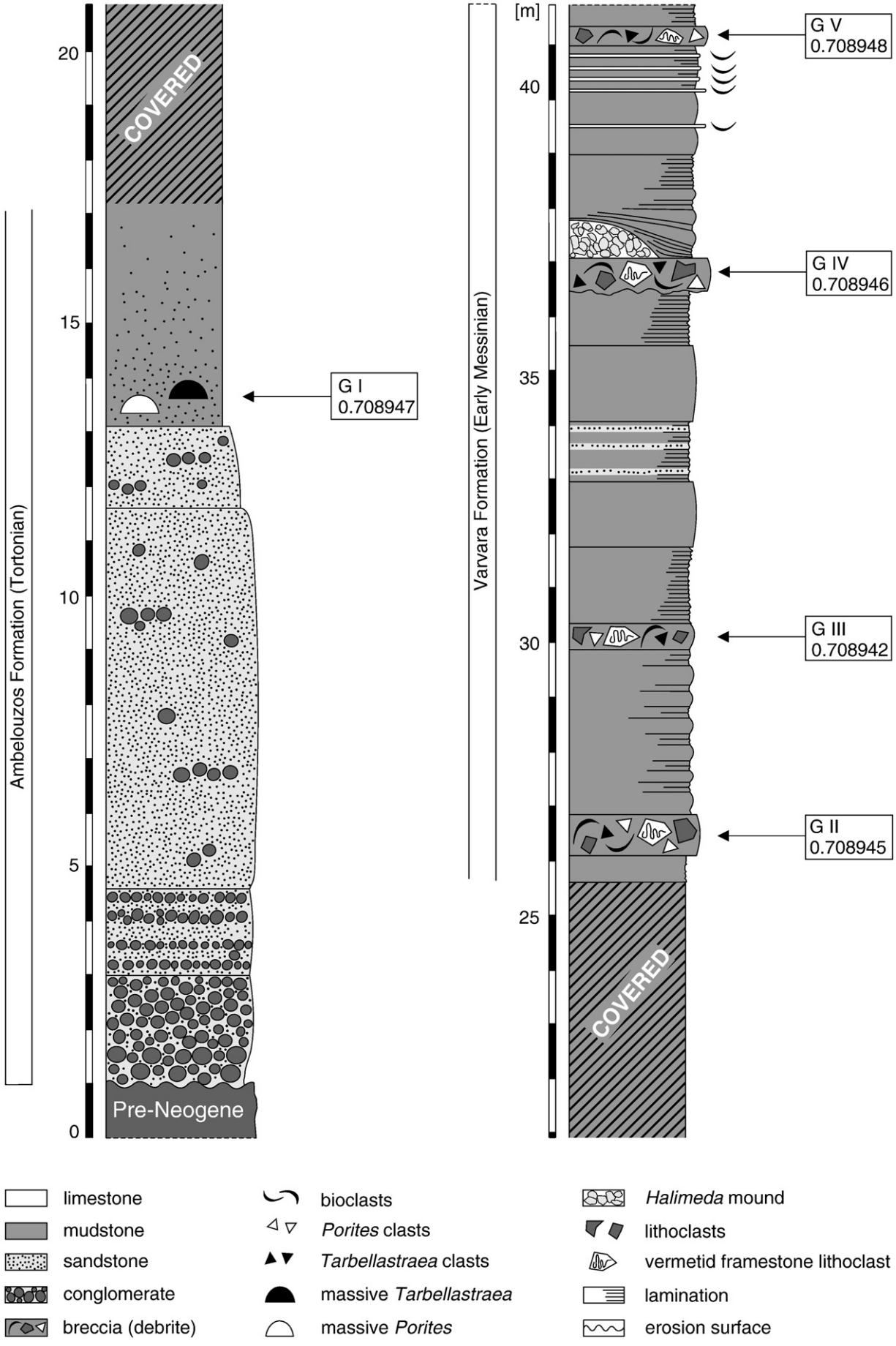

Table 1
Specimen number, sampling site code (P = Psalidha, G = Gorgolaini Monastery), mean $^{87}Sr/^{86}Sr$ ratios of each sampling site (2σ analytical error <0.000008), genus, length of obtained time series, mean $\delta^{18}O$ values, average $\delta^{18}O$ minima (summer) as well as maxima (winter), mean $\delta^{18}O$ amplitudes (seasonality) and average annual growth rate of the analyzed corals.

Specimen	Sampling level	$^{87}Sr/^{86}Sr$	Genus	Time series [years]	Mean $\delta^{18}O$ [‰]	Average $\delta^{18}O$ minima [‰]	Average $\delta^{18}O$ maxima [‰]	Mean $\delta^{18}O$ amplitudes [‰]	Annual growth rate [mm y^{-1}]	
P2[a]	P I	0.708917	*Porites*	66.7	−2.68	−3.11	−2.16	0.95	3.6	Tortonian
P16	P I		*Porites*	20.8	−2.74	−3.20	−2.07	1.08	3.4	
P1[a]	P II	0.708924	*Porites*	15.0	−2.76	−3.11	−2.20	0.91	4.9	
P3[a]	P II		*Porites*	3.7	−2.60	−3.08	−1.94	1.14	5.8	
P4[a]	P II		*Porites*	11.2	−2.95	−3.44	−2.28	1.16	4.5	
P7[b]	P II		*Tarbellastraea*	10.3	−2.53	−3.02	−2.03	0.99	3.3	
P8[b]	P II		*Porites*	16.6	−2.70	−3.08	−2.05	1.03	5.0	
P8B	P II		*Porites*	20.5	−2.44	−2.90	−1.75	1.15	5.7	
P9[b]	P II		*Porites*	17.8	−2.50	−3.00	−1.82	1.18	3.6	
P12	P III	0.708913	*Porites*	18.2	−3.42	−3.88	−2.67	1.21	5.3	
P14	P III		*Porites*	14.7	−3.23	−3.71	−2.46	1.25	4.7	
SF1	G I	0.708947	*Tarbellastraea*	15.0	−1.79	−1.98	−1.40	0.58	2.0	
SF2	G I		*Tarbellastraea*	10.0	−1.52	−1.70	−1.31	0.39	1.9	
SF3	G I		*Tarbellastraea*	–	−1.59	–	–	–	–	
SF4	G I		*Tarbellastraea*	–	−1.60	–	–	–	–	
SF5	G I		*Tarbellastraea*	–	−1.68	–	–	–	–	
MG9/2[b]	G II	0.708945	*Tarbellastraea*	42.2	−2.46	−2.82	−2.08	0.74	3.4	Messinian
MG9/4	G II		*Porites*	–	−2.41	–	–	–	–	
MG9/6	G II		*Tarbellastraea*	–	−2.35	–	–	–	3.0	
MG10-11/1	G III	0.708942	*Porites*	–	−2.53	–	–	–	3.0	
MG10-11/2	G III		*Porites*	–	−2.76	–	–	–	–	
MG10-11/3	G III		*Porites*	–	−2.21	–	–	–	3.8	
MG10-11/4	G III		*Porites*	2.0	−2.64	−2.96	−2.35	0.61	3.0	
MG10-11/5	G III		*Porites*	–	−2.70	–	–	–	–	
MG16/1	G IV	0.708946	*Porites*	–	−2.33	–	–	–	4.0	
MG16/2	G IV		*Tarbellastraea*	–	−2.44	–	–	–	–	
MG24/2	G V	0.708948	*Porites*	19.6	−1.65	−2.01	−1.35	0.66	4.3	
MG24/3	G V		*Tarbellastraea*	–	−1.56	–	–	–	3.1	

[a] Brachert et al. (2006a).
[b] Mertz-Kraus et al. (2008).

4.2. Radiogenic strontium isotope analyses

For bulk Sr isotope analyses approximately 150 µg of coral aragonite from each sampling site was reacted with 200 µl ultra-pure 1 M acetic acid. Additionally, 10 mg of gypsum from a locality (E 24.94829°, N 35.09817°) close to Apomarma north of Psalidha where laminated evaporites interfinger with the Messinian Varvara Formation (Reuter et al., 2005) and from a locality close to Sarhos (E 25.00198°, N 35.22118°) east of Kroussonas (Fig. 1), respectively, were dissolved with 1 ml ultra-pure 2.0 N HCl. Solutions were separated from residues by centrifugation, evaporated and redissolved in 200 µl 3 N HNO_3 and dried down again. Strontium was separated from the samples using EiChrom® Sr-spec resin, a Sr-selective extraction chromatographic resin (Horwitz et al., 1992). Teflon shrink columns (100 µl) packed with Sr-spec resin were preconditioned with 500 µl of 3 N HNO_3 and the samples loaded in 100 µl 3 N HNO_3. The samples were then washed in with three portions of 100 µl of 3 N HNO_3 followed by 3 ml of 3 N HNO_3. Sr was eluted with 1 ml of MilliQ water. The eluate was evaporated, transformed into a nitrate by adding 1 drop of concentrated HNO_3 and dried down. The Sr recovered (~100 ng) was loaded onto previously outgassed W single filaments together with a tantalum fluoride activator (Birck, 1986). The isotopic compositions were measured on a Triton TIMS instrument (ThermoFisher, Bremen) at the Max Planck-Institut für Chemie at Mainz. Regular measurements of the NIST SRM 987 Sr standard, measured in static mode, range from 0.710230 to 0.710259 ($n=32$) and are 0.710244 on average (2SD = 0.000013). In dynamic mode values range from 0.710245 to 0.710269 ($n=17$) and are 0.710257 on average (2SD=0.000012). Measured sample $^{87}Sr/^{86}Sr$ ratios were corrected to the NIST SRM 987 value of 0.710248 (McArthur et al., 2001). For all samples the internal analytical error is $<\pm 0.000008$ (2σ). Age estimations are based on Sprovieri et al. (2003) and Flecker et al. (2002).

4.3. Stable isotope analyses and data processing

Sample preparation for stable isotope analyses was done using a PROXXON micro miller equipped with a spherical bit (Ø 0.6 mm) operating at low speed. Equidistant sampling spots (distance of centers 0.8 mm) in *Porites* were aligned along the axis of maximum growth, as indicated by X-ray images. The drilling depth was kept constant at 1.5 mm. The sampling profile for *Tarbellastraea* followed the growth direction of one single corallite according to the method described in Mertz-Kraus et al. (2008). The sampling procedure provides an average of ≥4 samples per year due to the average annual growth rate of 3–5 mm (Brachert et al., 2006b, Table 1).

Stable oxygen and carbon isotope ratios were measured at the Institute of Geosciences, University of Frankfurt and at the Department of Geology and Mineralogy, University of Erlangen-Nürnberg (Germany). All values are reported in per mil relative to V-PDB. The internal analytical precision and external reproducibility was better than ±0.08‰ for $\delta^{18}O$ and $\delta^{13}C$ (1σ).

Annual density banding patterns visible in X-ray images are the basis for the age models of the $\delta^{18}O$ time series presented. The most positive $\delta^{18}O$ value in each annual cycle was considered to define the "winter" and was assigned as a tie point in the internal age model. The ages of the other sampling points between the winters were calculated by linear interpolation according to their position along the sampling transect. Mean seasonal $\delta^{18}O$ amplitudes of each coral were estimated as the average of the differences of all annual minima and maxima.

For each coral, an evenly spaced $\delta^{18}O$ time series was resampled at a bimonthly resolution, matching best with the original record, using the AnalySeries 2.0 software package (Paillard et al., 1996). Additionally, each time series was detrended linearly and normalized to unit variance. Spectral analysis of the coral $\delta^{18}O$ data was performed with

Fig. 3. Geological section at Gorgolaini Monastery including sampling sites G I (CL 4) of Tortonian age, G II (CL 7.1), G III, G IV (CL 7.2) and G V (CL 7.3) from the Early Messinian and respective mean $^{87}Sr/^{86}Sr$ values. CL nomenclature of Brachert et al. (2006b).

the kSpectra Toolkit 2.7 (SpectraWorks: http://www.kspectraworks.com) (Ghil et al., 2002). We applied the multi-taper method (MTM) (Thomson, 1982) with number of tapers set to 3, a bandwidth parameter of 2, and a red noise null hypothesis.

Mean annual $\delta^{18}O$ values were calculated as the average of six bimonthly interpolated values for a single year. The mean $\delta^{18}O$ value of one individual coral specimen is taken as the average of all annual mean values of this specimen. For estimation of SST variations from coral $\delta^{18}O$, we made use of the relationship between $\delta^{18}O_{aragonite}$ and temperature (0.15‰ per 1 °C) discussed by Felis et al. (2004). Additionally, the relationship between SSS and $\delta^{18}O_{seawater}$ is given by Pierre (1999) as:

$$SSS = \left(\delta^{18}O_{seawater} + 8.9\right) / 0.27 \quad (1)$$

which allows us to estimate differences in salinity (ΔSSS) between two samples A and B from:

$$\Delta SSS = \left(\delta^{18}O_{seawater\,A} - \delta^{18}O_{seawater\,B}\right) / 0.27 \quad (2)$$

where $\delta^{18}O_{seawater}$ in Eqs. (1) and (2) is expressed relative to SMOW. Applying the relationship between SST, $\delta^{18}O_{seawater}$ and $\delta^{18}O_{aragonite}$ given by Felis et al. (2004)

$$SST = 5.291 - 6.605 \times \left(\delta^{18}O_{aragonite} - \delta^{18}O_{seawater}\right) \quad (3)$$

and the relationship between PDB and SMOW units (Coplen et al., 1983), as well as the $\delta^{18}O_{aragonite}$-independent SST estimation based on the relationship between annual mean SST and annual growth rates (G), calculated using unpublished data provided by Janice Lough (Australian Institute of Marine Science, Townsville, Australia):

$$SST = 0.2683 \times G + 22.775 \quad (4)$$

we can transform Eq. (2) into

$$\Delta SSS = 3.818 \times \left(\delta^{18}O_{aragonite\,A-B} + 0.2683 \times G_{A-B} / 6.605\right) \quad (5)$$

which expresses the salinity difference as a function of the difference in coral $\delta^{18}O$ and growth rates in two samples. $\delta^{18}O_{aragonite\ A-B}$ and G_{A-B} are the absolute values of the differences of the parameters $\delta^{18}O_{aragonite}$ and G, respectively, between the two samples A and B. $\delta^{18}O_{aragonite\ A-B}$ is expressed relative to PDB.

A one-way analysis of variance (ANOVA) has been performed in order to compare the mean $\delta^{18}O$ values of corals from the eight sampling sites P I to G V. All values were transformed by $\log_{10}(x+1)$ to satisfy the homogeneity of variance assumptions. The tested null hypothesis H_o was that there are no statistically significant differences ($p>0.05$) in the mean $\delta^{18}O$ values among the different sampling sites against the alternate hypothesis H_1 that there are statistical describable differences ($p<0.05$).

5. Results

5.1. Radiogenic strontium isotope ratios

Sr isotope compositions of the coral aragonite were assigned to two different groups: The coral specimens analyzed from Tortonian sites P I, P II and P III have $^{87}Sr/^{86}Sr$ ratios ranging from 0.708900 to 0.708940 ($n=55$). Values from sites G I, G II, G III, G IV and G V differ clearly from the Tortonian values of P I to P III and range from 0.708932 to 0.708958 ($n=26$). In Table 1, Figs. 2 and 3, Tortonian and Messinian mean $^{87}Sr/^{86}Sr$ ratios of the coral aragonite for each sampling site are shown together with the respective stratigraphic positions within the sections. The gypsum sample analyzed have a mean $^{87}Sr/^{86}Sr$ value of 0.708956.

5.2. Stable oxygen isotope ratios

Oxygen isotope variations of corals from eight Late Miocene stratigraphic levels of Tortonian age (P I, P II, P III and G I) and Early Messinian age (G II, G III, G IV and G V) were compared. The data comprise 28 specimens of *Tarbellastraea* as well as *Porites*. Table 1 shows the analytical results of the new specimens along with results from previous publications. Oxygen isotope compositions of *Tarbellastraea* and *Porites* within a given coral level are statistically indistinguishable, and thus both genera represent compatible proxy archives (Mertz-Kraus et al., 2008). A minimum of four samples per year were taken, so that the resolution is at least quarterly. Unless otherwise noted, the sampling resolution was the same for all coral specimens analyzed. The sampled records represent 2 to 67 years of coral growth (Table 1). All corals analyzed yielded cyclic $\delta^{18}O$ signals corresponding to the annual density bands visible in X-ray images. For all sampling sites apart from G I, $\delta^{13}C$ is systematically phase-shifted relative to $\delta^{18}O$. Maxima in $\delta^{18}O$ coincide with high-density bands and minima with low-density bands. This yearly cyclicity was observed independent of the stratigraphic position of the sample; further in terms of statistics, values from corals that derive from the same stratigraphic level are identical. There are, however, significant differences in mean $\delta^{18}O$ values and mean seasonal $\delta^{18}O$ amplitudes in corals taken from different stratigraphic levels. Statistical evaluation of the mean $\delta^{18}O$ values was done applying ANOVA. The resulting p-values are indicated in Table 2.

5.2.1. Psalidha sampling sites

5.2.1.1. Site P I. On average, the annual $\delta^{18}O$ minima are −3.16‰ and the maxima −2.12‰, respectively, at sampling site P I. Mean $\delta^{18}O$ values range from −2.74‰ to −2.68‰ with an average of −2.71‰. Mean seasonal $\delta^{18}O$ amplitudes vary between 0.95‰ and

Table 2
p-values of one-way analysis of variance (ANOVA) on mean $\delta^{18}O$ values of corals from eight different sampling sites (see Table 1).

	Sampling level							
	P I	P II	P III	G I	G II	G III	G IV	G V
P I	–							
P II	0.59^{NS}	–						
P III	0.023^{S}	0.0022^{S}	–					
G I	0.000081^{S}	0.00000022^{S}	0.000018^{S}	–				
G II	0.0080^{S}	0.056^{NS}	0.0013^{S}	0.000040^{S}	–			
G III	0.43^{NS}	0.53^{NS}	0.010^{S}	0.000016^{S}	0.28^{NS}	–		
G IV	0.037^{S}	0.088^{NS}	0.012^{S}	0.00042^{S}	0.73^{NS}	0.33^{NS}	–	
G V	0.0029^{S}	0.000037^{S}	0.0030^{S}	0.72^{NS}	0.00062^{S}	0.0012^{S}	0.0081^{S}	–

NS: no significant difference ($p>0.05$) between corresponding sites.
S: significant difference ($p<0.05$) between corresponding sites.

1.08‰, and average 1.02‰. The 67-year record from *Porites* P2 (Fig. 4a) was obtained from the P I site in an earlier study, and these data have already been used for spectral analysis (Brachert et al., 2006a). However, to ensure compatible data processing, this multidecadal data set was reanalyzed for interannual variability. Significant spectral peaks were identified at periods of 2.2 and 4.7 years (Fig. 5a).

5.2.1.2. Site P II. At site P II, $\delta^{18}O$ data were obtained for seven coral specimens. On average, the annual $\delta^{18}O$ minima are −3.09‰ and the maxima −2.01‰, respectively. Mean $\delta^{18}O$ values range from −2.95‰ to −2.50‰ with an average of −2.64‰. Mean seasonal $\delta^{18}O$ amplitudes vary between 0.91‰ and 1.18‰, and average 1.08‰.

5.2.1.3. Site P III. Two *Porites* specimens from site P III yielded $\delta^{18}O$ records 18 (Fig. 4b) and 15 years long, respectively (see Table 1), with an average of all $\delta^{18}O$ minima of −3.80‰ and of all $\delta^{18}O$ maxima of −2.57‰. Mean $\delta^{18}O$ values range from −3.42 to −3.23‰ (−3.33‰ on average). Mean seasonal $\delta^{18}O$ amplitudes vary between 1.21‰ and 1.25‰, with an average value of 1.23‰.

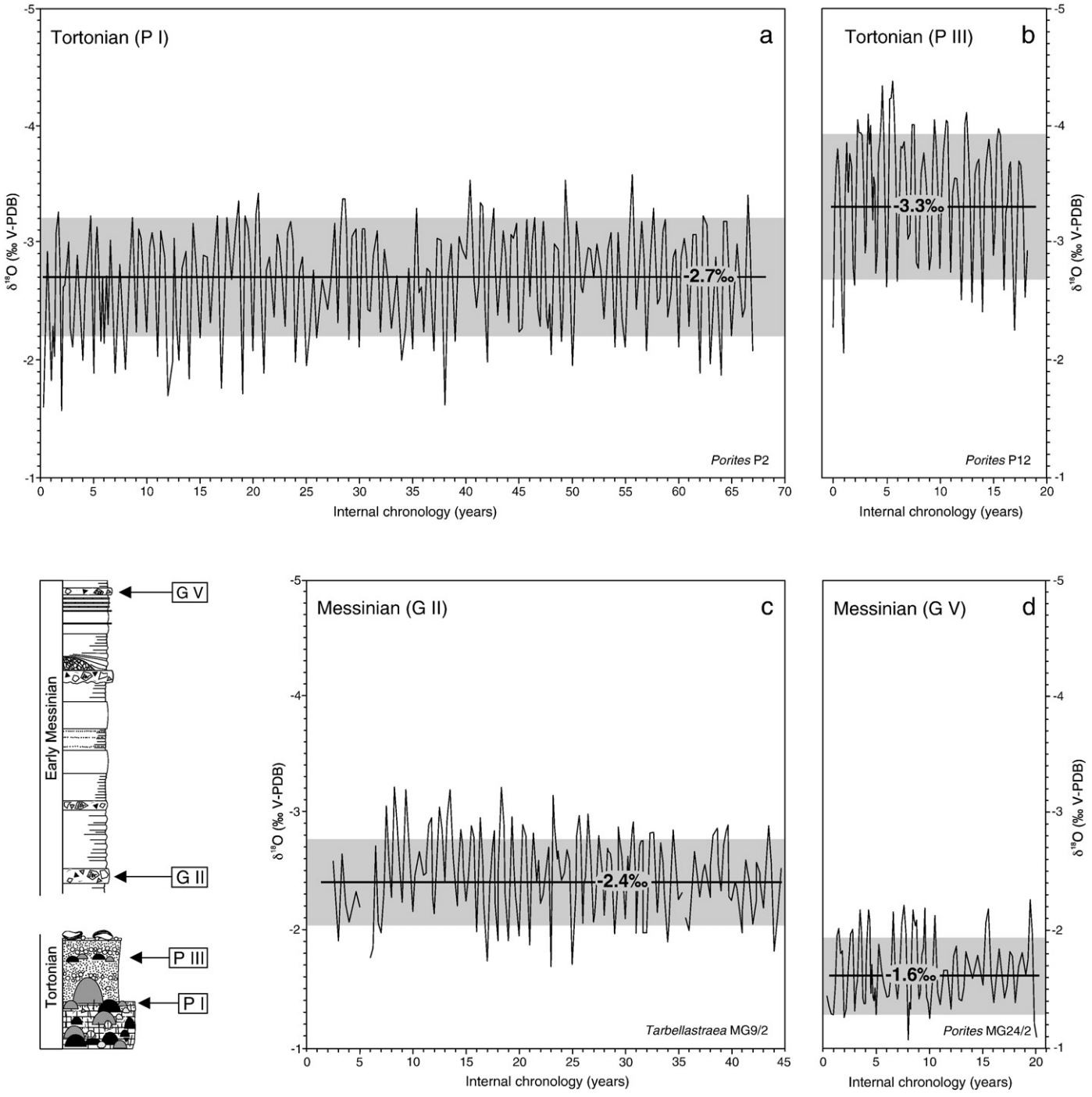

Fig. 4. Coral $\delta^{18}O$ records of the four sampling sites P I and P III (Tortonian) as well as G II and G V (Messinian). All $\delta^{18}O$ records show cyclic signals. Mean $\delta^{18}O$ values (horizontal line) differ between different sampling levels: (a) P I: −2.7‰, (b) P III: −3.3‰, (c) G II: −2.4‰ and (d) G V: −1.6‰. Mean seasonal $\delta^{18}O$ amplitudes (grey shading) are also variable, and vary between 1.23‰ (site P III) and 0.66‰ (site G V). In the bottom left-hand corner the geological section illustrates the stratigraphic position of the four sampling sites.

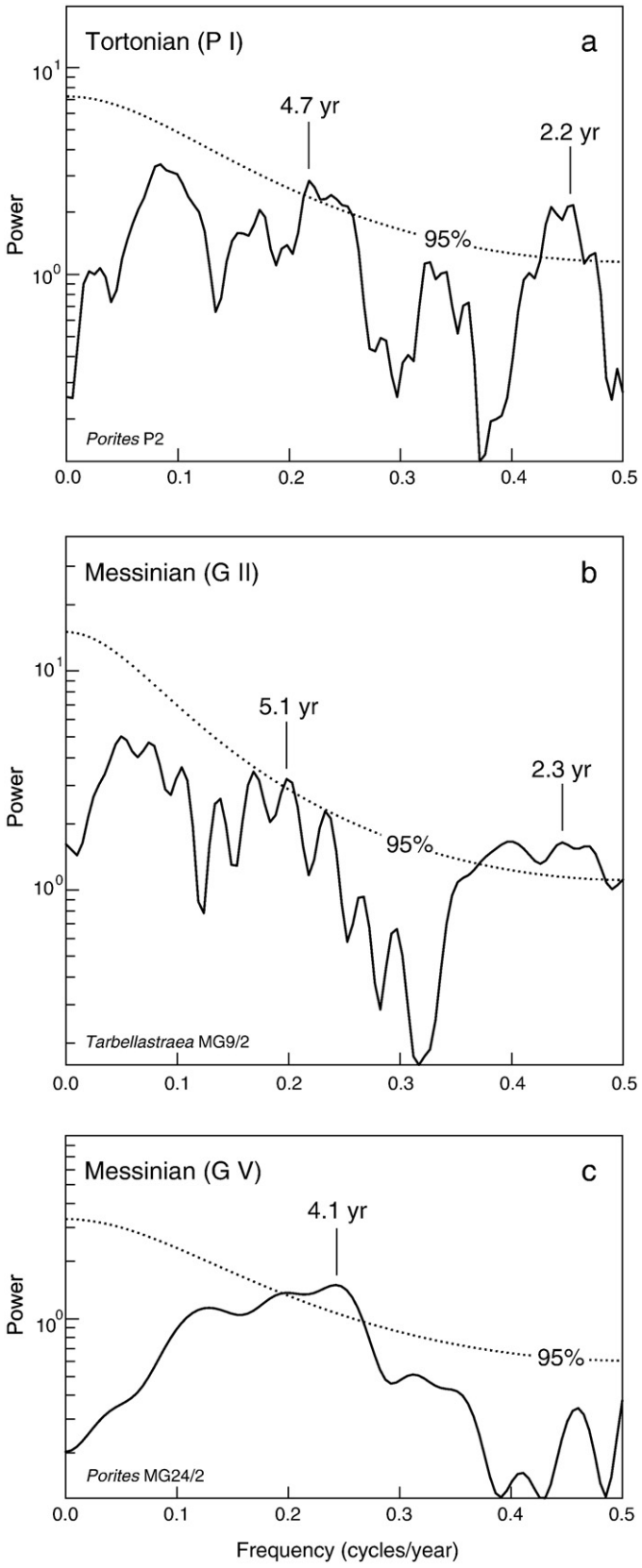

Fig. 5. Power spectra (MTM) of the Late Miocene coral $\delta^{18}O$ time series. (a) *Porites* P2 (67-year record, site P I, age ~10 Ma, Tortonian), (b) *Tarbellastraea* MG9/2 (42-year record, site G II, age ~7 Ma, Messinian), and (c) *Porites* MG24/2 (20-year record, site G V, age ~7 Ma, Messinian). Dotted lines indicate a 95% significance level. Significant periods are marked.

5.2.2. Gorgolaini Monastery sampling sites

5.2.2.1. Site G I. Two *Tarbellastraea* specimens (SF1 and SF2) from G I gave discontinuous transects of ca. 15 and 10 years, respectively. The mean seasonal $\delta^{18}O$ amplitudes vary between 0.58‰ and 0.39‰, with an average of 0.49‰. The average of all $\delta^{18}O$ minima is −1.84‰ and of all $\delta^{18}O$ maxima is −1.36‰. Together with three other discontinuously sampled *Tarbellastraea* specimens a mean $\delta^{18}O$ value of −1.64‰ was calculated for G I from the mean $\delta^{18}O$ values of the single specimen ranging from −1.52‰ to −1.79‰.

5.2.2.2. Site G II. Well-preserved *Porites* skeletal material within the lowermost Messinian level is present only within limited skeletal domains of one specimen. The resulting sampling transect is therefore short and discontinuous. For this reason, the mean $\delta^{18}O$ value (−2.41‰) was calculated by averaging the measured values of the *Porites* (MG9/4) analyzed. By analogy, for another coral specimen (*Tarbellastraea* MG9/6) a mean $\delta^{18}O$ value of −2.33‰ was obtained. From *Tarbellastraea* MG9/2 a 42-year record was reported previously (Mertz-Kraus et al., 2008) with an average of −2.82‰ for the minima and −2.08‰ for the maxima. The mean seasonal $\delta^{18}O$ amplitude is 0.74‰ (Fig. 4c). The mean $\delta^{18}O$ value of the G II data sets is −2.41‰. Significant spectral peaks exist at 2.3 and 5.1 years (Fig. 5b).

5.2.2.3. Site G III. A short 2-year transect of a *Porites* specimen (MG10-11/4) gives a mean seasonal $\delta^{18}O$ amplitude of 0.61‰ and an average of −2.96‰ for the $\delta^{18}O$ minima and −2.35‰ for the $\delta^{18}O$ maxima. From additional discontinuous sampling of four other *Porites* specimen mean $\delta^{18}O$ values were obtained, ranging from −2.76 to −2.21‰, with an average of −2.57‰.

5.2.2.4. Site G IV. In common with the G I site, the G IV site provided little well-preserved skeletal material. Sampling transects at G IV are short and discontinuous, and only allow mean $\delta^{18}O$ values from one *Porites* and one *Tarbellastraea* specimen to be obtained. Mean $\delta^{18}O$ values range from −2.44 to −2.33‰, while the average is −2.39‰.

5.2.2.5. Site G V. The uppermost sampling level yielded a 20-year record of *Porites* (specimen MG24/2) (Fig. 4d). The mean $\delta^{18}O$ value of this data set is −1.65‰ and the mean seasonal $\delta^{18}O$ amplitude is 0.66‰. The average of the minima is −2.01‰, while the average of the maxima is −1.35‰. Discontinuous sampling of a *Tarbellastraea* specimen (MG24/3) provided a mean $\delta^{18}O$ value of −1.56‰. Notwithstanding the relatively short 20-year chronology of MG24/2, spectral analysis of this record identified a significant peak at ~4 years (Fig. 5c).

6. Discussion

6.1. Radiogenic strontium isotope ratios

$^{87}Sr/^{86}Sr$ values from diagenetically unaltered biogenic carbonates are widely used to estimate ages of sedimentary successions based on the well-documented time-evolution of the Sr isotope composition of seawater (e.g., McArthur et al., 2001). The isotopic composition of Neogene seawater is well documented (e.g., Hodell et al., 1989) and allows successful application of this technique in restricted basins if there is sufficient mixing with the open ocean (Flecker et al., 2002; Flecker and Ellam, 2006). However, the chronostratigraphic resolution of the $^{87}Sr/^{86}Sr$ seawater curve for the Late Miocene is low because there are only small changes in $^{87}Sr/^{86}Sr$ over time (McArthur et al., 2001).

All $^{87}Sr/^{86}Sr$ values measured from Psalidha corals fall within the range of Tortonian Mediterranean seawater (e.g., Sprovieri et al., 2003) and are consistent with their relative stratigraphic position (Reuter et al., 2005). Therefore, an age of around 10 to 9 Ma is considered for the Psalidha sampling sites (P I to P III).

$^{87}Sr/^{86}Sr$ data from corals of the Gorgolaini section cluster around 0.708946 and are consistent with published ranges from astronomically calibrated foraminifera samples from the island of Gavdos south of Crete that are assumed to reflect open Messinian ocean water (Flecker et al., 2002).

The Sr isotope ratios of the gypsum samples from the Varvara Formation at Apomarma and Sarhos, assigned to the Early Messinian (Meulenkamp et al., 1979), fit well with published values of the Lower Evaporites, which have a Sr isotope signature of Messinian open ocean water (Flecker et al., 2002). Since the Apomara evaporites interfinger with sediments of the Varvara Formation, a Messinian age for the debrites of the Varvara Formation at Gorgolaini Monastery appears conclusive. Therefore, the measured Sr isotope ratios imply an age of around 6.5 to 7.5 Ma for the Gorgolaini section. In combination with lithological evidences an Early Messinian age is assigned to the debrites (sites G II to G V) and a Late Tortonian age to the sampling site G I.

6.2. Mean annual $\delta^{18}O$ compositions

Average annual stable oxygen isotope compositions of corals (*Porites*, *Tarbellastraea*) show considerable variation among the eight sampling levels (Fig. 6). One-way analysis of variance yield statistically significant differences ($p<0.05$) between the mean $\delta^{18}O$ values of coral sampling sites, e.g., between P I/P II and P III, P I/P II and G I, P I/P II and G V, P III and G I, as well as P III and G V (Table 2). There are also statistically indistinguishable sampling sites ($p>0.05$) which are not considered in deriving SST or SSS variations.

Intermediate mean $\delta^{18}O$ compositions were found at levels P I and P II of Psalidha section (−2.71‰ and −2.64‰), and G II through G IV of Moni Gogolaini section (−2.41‰, −2.57‰ and −2.39‰). Substantial excursions, however, exists at P III representing the most negative composition (−3.33‰) and G I and G V representing the most positive values (−1.64‰ and −1.61‰), respectively. The difference in mean $\delta^{18}O$ between Tortonian P I and the uppermost Messinian G V on average is 1.10‰, and has a maximum of 1.72‰ between P III and G V (Table 1, Fig. 6). Between P I and P III the difference is 0.62‰, between P II and P III 0.69‰, and 1.69‰ between P III and G I.

In modern corals, variations in SST are usually derived using a local, empirical relationship between SST and $\delta^{18}O_{aragonite}$. Such relationships are not well known for ancient corals. For this reason, we have used the SST–$\delta^{18}O$ relationship published for modern *Porites* from the Red Sea (Felis et al., 2004) for the Late Miocene Mediterranean corals. This appears to be justified because the oceanographic setting of the current Red Sea and Late Miocene Eastern Mediterranean Sea are comparable.

If we assume SST to control exclusively the variations in coral $\delta^{18}O$, the shift of 0.62‰ or 0.69‰ between the Tortonian sampling sites P I and P III, or P II and P III, respectively, would imply a SST increase of 4.1 °C or 4.6 °C within a few meters of the geological section. The more positive values from P III to G I imply a SST decrease of 11.2 °C. Additionally, the general shift to more positive mean $\delta^{18}O$ values implies a decrease in SST of 7.3 °C from the Tortonian P I to the Messinian G V, or 11.4 °C from the Tortonian P III to the Messinian G V (Fig. 6). Such implied temperature changes are extreme and unfounded. For this reason, we do not consider that the long-term variations in coral $\delta^{18}O$ can be simply related to changes in SST. Below, we consider the arguments in more detail.

Although reef growth occurred in the Late Miocene almost over the entire Mediterranean region (e.g., Esteban, 1979; Reuter et al., 2006), it was rather discontinuous. The coral fauna was of low diversity and dominated by two genera: *Porites* and *Tarbellastraea* (Brachert et al., 1996; Bosellini and Perrin, 2008). In concert with low growth rates of ~3 to 5 mm yr^{-1} in massive *Porites*, the distribution and diversity fit suggestions that average winter SSTs were near the lower threshold for reef coral growth in the Tortonian as well as in the Messinian (Brachert et al., 2006a). This estimate is in agreement with the distributional patterns of modern coral reefs, which are limited by minimum long-term winter SST < 18 °C, though some short excursions below this temperature may occur (Veron and Minchin, 1992; Abram et al., 2001). Average annual SSTs of 23 °C and average winter SST around 20 °C for the Eastern Mediterranean during the Late Miocene were derived from coral growth rates (Brachert et al., 2006b). However, biofacies analysis has revealed SST below the critical threshold temperature during some stratigraphic intervals without coral growth (Kroeger et al., 2006). SST estimates based on the taxonomic richness of coral reef assemblages at a given locality (Rosen, 1999) also imply constant winter SSTs around 19 °C since the number of coral genera is almost unchanged in the Mediterranean sampling sites of Tortonian and Messinian age (Bosellini and Perrin, 2008). Another important line of evidence is that foraminiferal assemblages indicate mild winter temperatures in the Messinian (Perez-Folgado et al., 2003). Therefore, severely increasing SSTs during the Tortonian as well as drastically decreasing SSTs towards the Messinian appear questionable considering the stratigraphic intervals containing coral assemblages.

One might argue, therefore, that measured mean $\delta^{18}O_{aragonite}$ variability is caused by compositional changes in $\delta^{18}O$ of global ocean water, such as in response to changing ice volume. On balance, this appears a much more promising explanation of our results. However, a 0.1‰ change in global ocean water $\delta^{18}O$ can be considered equivalent to a ~10 m eustatic change (Miller et al., 2005) or 60 to 70 m of sea-level rise from PI/PII to PIII or a 160 m sea-level fall from P III to G I. Such drastic changes in sea level are not supported by sedimentary facies analysis. There is no correspondence in the compositional changes in $\delta^{18}O$ of global ocean water to the more negative $\delta^{18}O_{aragonite}$ between P I and P III, or P II and P III, respectively. Nonetheless, the change in $\delta^{18}O_{aragonite}$ between the Tortonian P III and G I to more positive values coincides with an observed increase in $\delta^{18}O_{seawater}$ of around 0.5‰ at 8.2 Ma (Miller et al. (2005). However, this increase in $\delta^{18}O_{seawater}$ is small compared to the coral aragonite data — the change from P III to G I in $\delta^{18}O_{aragonite}$ is higher by at least a factor of 3 than the change at 8.2 Ma in global mean $\delta^{18}O_{seawater}$. Furthermore, the reported shift in the global mean $\delta^{18}O_{seawater}$ record is of quite short duration and shows no long-term trend towards more positive $\delta^{18}O_{seawater}$ values during the Late Miocene.

The G I data set with more positive $\delta^{18}O_{aragonite}$ values and to some extent in-phase $\delta^{13}C$ patterns can be explained following Rosenfeld et al. (2003) as a coral community growing in deeper water. This assumption is confirmed by sandy marls indicating greater water depths, and low coral growth rates of <2.3 mm on average (Brachert et al., 2006b). The growth rate can be attributed therefore to low-light conditions (water depth and turbidity). Therefore the G I corals appear not to correspond with the pattern shown by the other sampling sites which are all associated with shallow waters.

For the coarse-grained delta deposits above P I we assume the changes towards more negative $\delta^{18}O_{aragonite}$ values in the Tortonian section (P I to P III) are more likely to reflect variability in local freshwater discharge and salinity of the ambient seawater, instead of substantial SST increase and global mean $\delta^{18}O_{seawater}$ variations. Using Eq. (5) of Section 4.3, the measured difference between P I and P III, or P II and P III in mean $\delta^{18}O_{aragonite}$ corresponds with an SSS decrease of 2.6‰ or 2.7‰, respectively. Such differences in SSS have been reported from sampling sites with open marine compared to estuarine-coastal environments (Akagi et al., 2004). Additionally, a major positive shift of 0.78‰ in coral mean $\delta^{18}O$ occurred at ~7 Ma (between G IV and G V), for which no equivalent excursion exists in the record of Miller et al. (2005). If this change could be related to eustatic sea-level change, a fall of about 70 m from G IV to G V or even 170 m from P III to G V would be the consequence. This has no equivalent in the sedimentary succession. Rather a long-term sea-level rise is assumed during the Late Miocene (Miller et al., 2005, André W. Droxler (Rice University, Houston), personal communication 2006). Therefore, ice volume change appears not to be the exclusive cause for the decrease of coral $\delta^{18}O$ from P I and P II to P III or the increase from P I to G V.

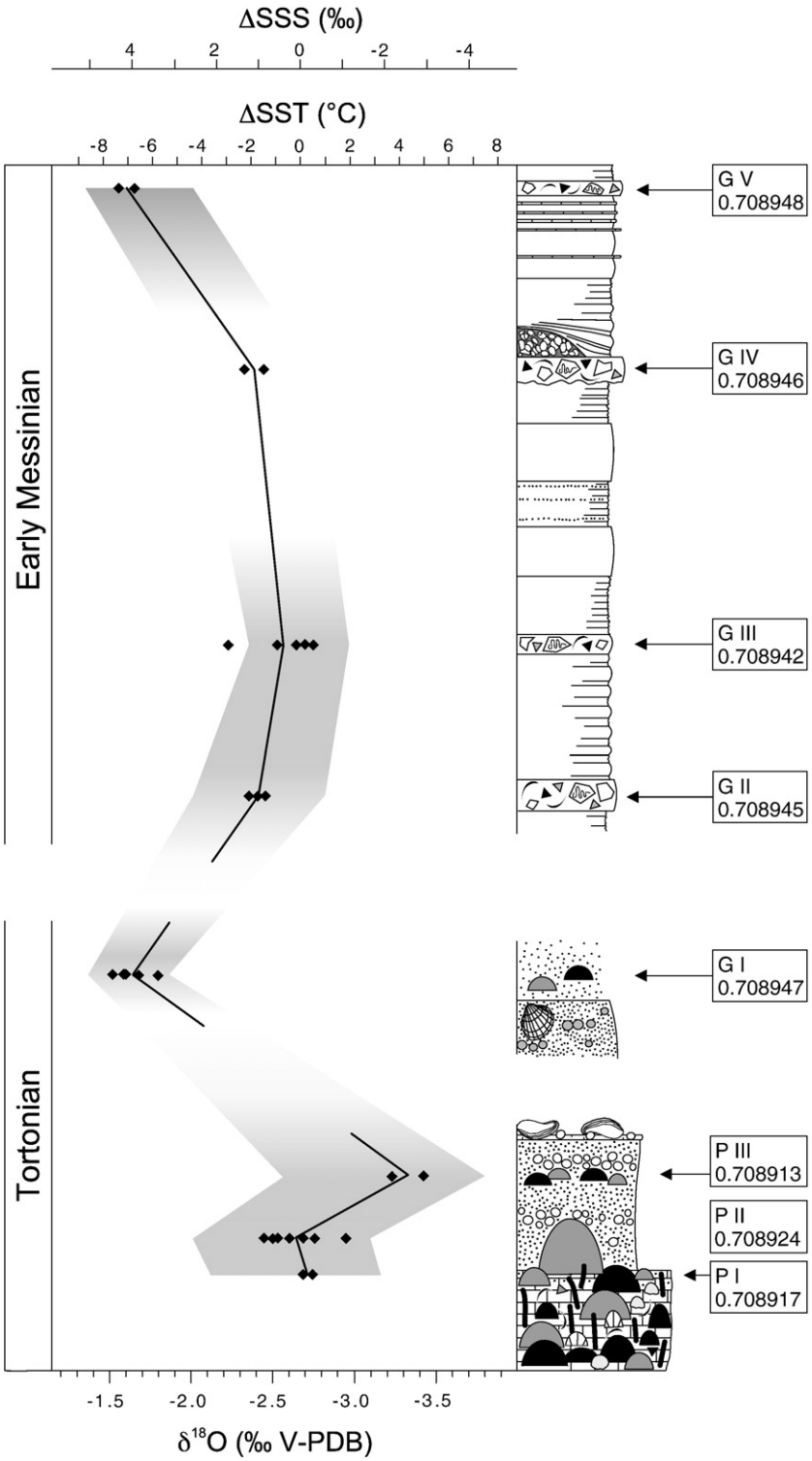

Fig. 6. Average of the mean $\delta^{18}O_{coral}$ values (black line) and averaged mean seasonal $\delta^{18}O_{coral}$ amplitudes (gray shading) of the eight sampling sites (P I to P III and G I to G V). The border of the shading illustrates the average $\delta^{18}O_{coral}$ maxima (winter) and minima (summer) values of each sampling site. Calculated SST and SSS variations are given relative to sampling site P I (chosen arbitrarily as zero point on the SST and SSS scale) and assume no global $\delta^{18}O_{seawater}$ change. Black diamonds represent mean $\delta^{18}O_{coral}$ values (Table 1) of the analyzed specimens. Mean $^{87}Sr/^{86}Sr$ values of each sampling site are indicated at the respective part of the section.

Increasingly positive, and also more variable $\delta^{18}O$ values starting at 6.7 (Blanc-Valleron et al., 2002) and 7.1 Ma (Kouwenhoven et al., 1999) have been reported and interpreted to be related to the uplift in the Betic Corridor area (Southern Spain). On the basis of progressive isolation of the Mediterranean basin, we assume that changing $\delta^{18}O$ values of sea surface water due to variable precipitation, river discharge and evaporation seem to be the predominant cause of the variability of $\delta^{18}O$ in the corals.

Paleobotanical and sedimentological data indicate a gradual shift from humid conditions (Reuter and Brachert, 2007), with annual precipitation rates of 1000 to 1200 mm (Sachse and Mohr, 1996; Zidianakis et al., 2004), to drier conditions, with annual precipitation rates of 400 to 500 mm (Fauquette et al., 2006) from the Tortonian to the Messinian. This observation, together with results from fossil mammal communities (Eronen et al., submitted for publication) and

almost constant growth rates in *Porites* and *Tarbellastraea* as well as non-variable coral diversity are all consistent with uniform SST during periods of coral growth (Rosen, 1999; Brachert et al., 2006b; Bosellini and Perrin, 2008). Thus, overall, our $\delta^{18}O_{aragonite}$ data appear to reflect predominantly effects of changes in salinity. Based on a modern Mediterranean $\delta^{18}O_{seawater}$–salinity relationship (Pierre, 1999), and using Eq. (5) of Section 4.3 we suggest the $\delta^{18}O$ data of the Late Miocene corals to indicate a minimum long-term salinity build-up in the marine Neogene Basins of Crete prior to the MSC of 2.3‰. Here, we have considered the ~0.5‰ change in $\delta^{18}O_{seawater}$ at 8.2 Ma reported by Miller et al. (2005) and subtracted this from the measured $\delta^{18}O$ shift of the Tortonian and Messinian corals. Alternatively, the salinity increase might have been as large as 6.8‰ (Fig. 6) if the ice-volume effect is considered to be only of subordinate relevance, and if we use the maximum difference of the $\delta^{18}O_{aragonite}$ values between P III and G V as a basis of the calculation. A difference of around 6‰ corresponds to that of SSS values of the modern northern Red Sea(~41‰) compared to open ocean waters (~35‰).

6.3. Mean seasonal $\delta^{18}O$ amplitudes

The lower mean seasonal $\delta^{18}O_{aragonite}$ amplitudes of 0.66‰ to 0.74‰ in the Messinian records compared to 0.91‰ to 1.25‰ in the Tortonian records (Table 1, Figs. 4 and 6) cannot be explained as an artifact of lower sampling resolution in the Messinian corals. The reason for this is that annual growth rates were similar in Tortonian and Messinian corals and sampling procedures were the same for all corals analyzed.

Early Tortonian mean seasonal $\delta^{18}O$ amplitudes in *Porites* and *Tarbellastraea* at Psalidha (P I to P III) correspond to 6.3 to 8.3 °C (7.2 °C on average) seasonal SST change (Fig. 6). Such SST seasonality is in agreement with modern SST seasonality of ca. 8 to 9 °C for the present-day Eastern Mediterranean (Brasseur et al., 1996; Poulos et al., 1997).

Rosenfeld et al. (2003) observed increasing seasonal $\delta^{18}O$ amplitudes in *Porites* growing in deep water caused by kinetic fractionation resulting in a correlation of $\delta^{18}O$ and $\delta^{13}C$ due to low extension rates. This pattern is not detectable in the stable isotope data of G I. Therefore, we explain the low seasonal $\delta^{18}O$ amplitudes of the corals from this level possibly as a result of the low annual extension rate of <2 mm which do not permit an appropriate sample resolution for defining the full range of seasonality between summer and winter in deeper water. Alternatively, seasonal differences in water temperature are less pronounced in deeper waters. Summarizing, the seasonal $\delta^{18}O$ amplitudes of G I corals do not provide reasonable information on seasonal variations in sea surface conditions.

Early Messinian mean seasonal $\delta^{18}O$ amplitudes (0.61‰ to 0.74‰) found in corals from the Gorgolaini Monastery section (G II, G III and G V) are substantially smaller than those of the Psalidha section. The amplitudes translate into a 4 °C to 5 °C seasonal SST change (Fig. 6), assuming the seasonal $\delta^{18}O_{aragonite}$ variability was exclusively controlled by temperature. If the estimated seasonal SST variations were the sole origin for observed seasonal $\delta^{18}O_{aragonite}$ changes, winter SSTs would have been cooler during the Tortonian (10 to 9 Ma) compared to those in the Messinian (~7 Ma). However, enhanced evaporation during summer or increased precipitation during winter, also influence surface water $\delta^{18}O$. Thus, the reduced mean seasonal $\delta^{18}O_{aragonite}$ amplitudes in the Messinian are most probably related to salinity changes.

Lowering the mean seasonal $\delta^{18}O$ amplitudes by increased precipitation during the Messinian winters would cause a shift of the mean $\delta^{18}O$ to more negative values which is in contrast to the measured Messinian data with more positive mean $\delta^{18}O$ compared to the Tortonian. In fact, the $\delta^{18}O$ values of the winter month are less affected than the summer $\delta^{18}O$ values. If disregarding the $\delta^{18}O$ values of P III, which we assume to reflect substantial freshwater input, and G I, the average winter $\delta^{18}O$ values from P I to G II are almost constant; only the summer $\delta^{18}O$ values are more positive by 0.3‰. From G II to G V the winter values are also more positive by 0.7‰, while the summer values continue to become more positive by 0.8‰. Therefore, we conclude that the Tortonian climate was generally more humid compared to the Messinian. Enhanced summer evaporation started in the earliest Messinian and intensified in the course of the Early Messinian when winters also became less humid in comparison to the Tortonian. Consequently, the shift to more positive mean $\delta^{18}O_{aragonite}$ coupled with lower seasonal $\delta^{18}O_{aragonite}$ amplitudes is mainly caused by enhanced summer evaporation.

If mean seasonal $\delta^{18}O$ amplitudes of Late Miocene coral aragonite were only influenced by seasonal salinity change, we estimate the average SSS seasonality to have been 4.2‰ during the Tortonian (P I to P III) and 2.8‰ or 2.3‰ during the Messinian (G III and G V), respectively (Eq. (5) of Section 4.3) (Fig. 6). In the present-day Aegean Sea, seasonal SSS variations at a given locality are ≤2‰ (Brasseur et al., 1996; Poulos et al., 1997) and far less than we infer for the Tortonian. Note that modern Aegean SSS variations correspond to seasonal $\delta^{18}O_{seawater}$ variations of ~0.5‰ (Eq. (2) of Section 4.3.). For this reason, a SSS seasonality in the Tortonian of >4‰ appears unlikely. Instead, we conclude that Tortonian mean seasonal $\delta^{18}O_{aragonite}$ amplitudes were mainly controlled by seasonal SST variability, with only minor contribution related to SSS seasonality. Recent climate modelling of the Late Miocene summer precipitation anomaly (model ECHAM4/ML) (G. Lohmann and A. Micheels, personal communication) has shown enhanced summer drought over the Mediterranean region. Thus, we suggest that the mean seasonal $\delta^{18}O_{aragonite}$ amplitudes present a mixed signal of SST and SSS, and especially so in the Early Messinian. This is in agreement with assumptions that the Mediterranean-type climate with dry summers occurred already in the Late Miocene in response to the uplift of the Himalaya–Tibetan plateau above a critical threshold (Tzedakis, 2007). Strong evaporation and thus high salinity during Eastern Mediterranean summers appear to account for the lower mean seasonal $\delta^{18}O_{aragonite}$ amplitudes at constant annual mean SST and Tortonian-like SST seasonality during the Early Messinian. Seasonality in SSS might be 1.5‰ higher (0.4‰ difference in mean seasonal $\delta^{18}O_{aragonite}$ amplitudes between Tortonian and Messinian data) in the Messinian than in the Tortonian assuming constant SST seasonality. This conclusion is consistent with increasing restriction of the Mediterranean during the Late Miocene, leading to the onset of the MSC at 5.96 Ma (Krijgsman et al., 1999).

The occurrence of increasing mean annual salinity together with pronounced SSS seasonality from the Tortonian to the Early Messinian is also supported by $\delta^{18}O$ data from marine inorganic aragonite precipitates (Brachert et al., 2007). These $\delta^{18}O$ data imply short events of enhanced salinity (>50‰) followed by the return to normal marine conditions suitable for coral reef growth. Brachert et al. (2007) concluded that salinity was highly variable more than 1 Myr prior to the MSC, and most likely the restricted basin structure intensified the patterns of precipitation, evaporation and therefore salinity distribution. Strong changes in water balance caused by isolation of the Mediterranean basin were similarly inferred to have taken place from foraminiferal stable oxygen isotope data by Sánchez-Almazo et al. (2007).

6.4. Spectral analysis

Data from three corals have $\delta^{18}O$ chronologies of sufficient length and resolution for analyzing interannual variability by spectral analysis. Multi-taper method (MTM) spectral analyses of these $\delta^{18}O$ time series show significant peaks at periods of 2–3 years and 4–5 years (Fig. 5). Identical spectral patterns have been found in a Late Pliocene coral $\delta^{18}O$ record from Florida (Roulier and Quinn, 1995). Likewise, Middle Miocene tree-ring data from Germany possess similar spectral peaks (Kurths et al., 1993). Additionally, last interglacial, late Holocene and modern proxy records of *Porites* from the Middle East (Felis et al., 2004) show similar peaks to those found in our data sets. Felis et al. (2000, 2004) inferred that the observed ~2

and ~5 year periods in *Porites* were related to fluctuations in the El Niño-Southern Oscillation (ENSO) and the North Atlantic Oscillation/Arctic Oscillation (NAO/AO).

Previous time series spectra from a Late Miocene coral (Brachert et al., 2006a) are confirmed by the MTM analysis here. On the basis of the spectral similarities, 10 Ma Tortonian and present-day atmospheric pressure fields are considered to be comparable comprising an Icelandic Low-type and an Azores High-type pressure center. These two pressure centers then control NAO/AO indices, though they would be located farther southward in the Tortonian (Brachert et al., 2006a). In the Tortonian, atmospheric variability of the pressure fields over the Northern Hemisphere influenced temperature as well as the hydrological balance: During periods with a positive NAO-type index, warm and humid air masses from the Atlantic reached the Mediterranean, whereas during periods with a negative NAO-type index, dry continental air came in from Northern Arabia. Our new time-series spectra of $\delta^{18}O$ show that the atmospheric variability during the Messinian at 7 Ma and the Tortonian at 10 Ma also was broadly similar. Interannual variation in $\delta^{18}O_{aragonite}$ in all the analyzed data sets shows peaks around 2 and 5 years. This indicates that a NAO-type interannual atmospheric variability is a rather stable and geologically old climate phenomenon, already occurring continuously or episodically during the Late Miocene.

7. Conclusions

Late Miocene corals from Crete (Eastern Mediterranean) show a significant change in mean annual $\delta^{18}O_{aragonite}$ values as well as in mean seasonal $\delta^{18}O_{aragonite}$ amplitudes during the time period from the Tortonian (10–9 Ma) to the Early Messinian (~7 Ma).

Mean $\delta^{18}O$ compositions of the Tortonian corals are up to 1.7‰ more negative than those from the uppermost Early Messinian sampling level, with a major shift to more positive values occurring at around 7 Ma ago. The change in mean $\delta^{18}O$ could be explained solely by a 7 to 11 °C decrease in SST. However, such a massive temperature decrease is not reasonable compared to other Late Miocene data from previous studies which document almost constant SSTs for Late Miocene episodes of coral growth. Furthermore, such a reconstruction would imply that during the Early Messinian the lower threshold SST of 18 °C for coral reef growth would have been clearly undercut by such a drastic SST decrease. The $\delta^{18}O$ records of the Late Miocene corals are, therefore, responding primarily to signals other than SST, such as $\delta^{18}O$ composition of seawater. The influence of ice-volume induced change in global $\delta^{18}O_{seawater}$ and sea-level change is not conclusive. The difference in mean $\delta^{18}O_{coral}$ of 1.7‰ would be equivalent to a sea-level fall of ~170 m from the Tortonian (site P III) to the Messinian (site G V). Lithological, paleobotanical and geochemical evidence supports $\delta^{18}O$ variation in the corals to result from SSS changes during the Late Miocene as a prelude to the MSC.

Mean seasonal $\delta^{18}O_{aragonite}$ amplitudes are 1.1‰ on average at 10–9 Ma and 0.7‰ at ~7 Ma. Since summer and winter $\delta^{18}O$ values are affected differently, we conclude that enhanced summer evaporation during the Early Messinian was the essential reason for lower $\delta^{18}O$ amplitudes and consequently more positive mean $\delta^{18}O$ indicating an ≥2‰ increase of annual mean SSS from the Tortonian to the Messinian.

Spectral analyses (MTM) of the Tortonian and the Messinian $\delta^{18}O$ chronological records indicate significant interannual variability with periods of 2–3 years and 4–5 years. Similarities in period compared to time series analyses of modern and other fossil proxy archives suggest an overall response to atmospheric forcing, in particular effects similar to the modern NAO/AO. This implies an atmospheric pressure field system with Iceland Low-type and Azores High-type pressure centers influencing climate conditions in the Circum-Mediterranean region at 10–9 Ma and ~7 Ma as much as at present-day. Our new $\delta^{18}O$ data from corals, therefore, suggest that the NAO/AO-type atmospheric pressure field phenomenon has been a robust feature over geologically significant periods of time.

Acknowledgements

We gratefully acknowledge J. Fiebig (Johann Wolfgang Goethe-Universität Frankfurt, Germany) and M. Joachimski (Friedrich-Alexander-Universität Erlangen-Nürnberg, Germany) for measuring the oxygen isotope ratios, H. Feldmann (Max-Planck-Institut für Chemie, Mainz, Germany) for technical support with solid-source mass spectrometry, H.-D. Werner and B. Schöne (Johannes Gutenberg-Universität Mainz, Germany) for access to XRD and sample preparation facilities, respectively, as well as J. Lough (Australian Institute of Marine Science, Townsville, Australia) for providing unpublished data. We highly appreciate constructive comments of an anonymous referee and D. Rickard (editor). This project was funded by the Deutsche Forschungsgemeinschaft (DFG, Germany) via grant BR 1153/9-3.

References

Abram, N.J., Webster, J.M., Davies, P.J., Dullo, W.C., 2001. Biological response of coral reefs to sea surface temperature variation: evidence from the raised Holocene reefs of Kikai-jima (Ryukyu Islands, Japan). Coral Reefs 20, 221–234.

Akagi, T., Hashimoto, Y., Fu, F.-F., Tsuno, H., Tao, H., Nakano, Y., 2004. Variation of the distribution coefficients of rare earth elements in modern coral-lattices: species and site dependencies. Geochimica et Cosmochimica Acta 68 (10), 2265–2273.

Billups, K., Schrag, D.P., 2003. Application of benthic foraminiferal Mg/Ca ratios to questions of Cenozoic climate change. Earth and Planetary Science Letters 209, 181–195.

Birck, J.-L., 1986. Precision K–Rb–Sr isotopic analysis: application to Rb–Sr chronology. Chemical Geology 56, 73–83.

Blanc-Valleron, M.-M., Pierre, C., Caulet, J.P., Caruso, A., Rouchy, J.M., Cespuglio, G., Sprovieri, R., Pestra, S., di Stefano, E., 2002. Sedimentary, stable isotope and micropaleontological records of paleoceanographic change in the Messinian Tripoli Formation (Sicily, Italy). Palaeogeography, Palaeoclimatology, Palaeoecology 185, 255–286.

Bosellini, F.R., Perrin, C., 2008. Estimating Mediterranean Oligocene–Miocene sea-surface temperatures: an approach based on coral taxonomic richness. Palaeogeography, Palaeoclimatology, Palaeoecology 258 (1–2), 71–88.

Brachert, T.C., Betzler, C., Braga, J.C., Martín, J.M., 1996. Record of climatic change in neritic carbonates: turnovers in biogenic associations and depositional modes (Upper Miocene, southern Spain). Geologische Rundschau 85, 327–337.

Brachert, T.C., Reuter, M., Felis, T., Kroeger, K.F., Lohmann, G., Micheels, A., Fassoulas, C., 2006a. *Porites* corals from Crete (Greece) open a window into Late Miocene (10 Ma) seasonal and interannual climate variability. Earth and Planetary Science Letters 245, 81–94.

Brachert, T.C., Reuter, M., Kroeger, K.F., Lough, J., 2006b. Coral growth bands: a new and easy to use paleothermometer in paleoenvironment analysis and paleoceanography (late Miocene, Greece). Paleoceanography 21, PA4217.

Brachert, T.C., Vescogni, A., Bosellini, F.R., Reuter, M., Mertz-Kraus, R., 2007. High salinity variability during the early Messinian revealed by stable isotope signatures from vermetid and *Halimeda* reefs of the Mediterranean region. Geologica Romana 40, 1–16.

Brasseur, P., Beckers, J.M., Brankart, J.M., Schoenauen, R., 1996. Seasonal temperature and salinity fields in the Mediterranean Sea: climatological analyses of a historical data set. Deep Sea Research Part I: Oceanographic Research Papers, vol. 43(2), pp. 159–192.

Coplen, T.B., Kendall, C., Hopple, J., 1983. Comparison of stable isotope reference standards. Nature 302, 236–238.

Druffel, E.R.M., 1997. Geochemistry of corals: proxies of past ocean chemistry, ocean circulation, and climate. Proceedings of the National Academy of Sciences of the United States of America 94, 8354–8361.

Eronen, J.T., Mirzaie, M., Karme, A., Micheels, A., Bernor, R.L., Fortelius, M., submitted for publication. Distribution History and Climatic Controls of the Late Miocene Pikermian Chronofauna. PNAS.

Esteban, M., 1979. Significance of the upper Miocene reefs of the western Mediterranean. Palaeogeography, Palaeoclimatology, Palaeoecology 29, 169–188.

Esteban, M., 1996. An overview of Miocene reefs from Mediterranean areas: general trends and facies models. In: Franseen, E.K., Esteban, M., Ward, W.C., Rouchy, J.-M. (Eds.), Models for Carbonate Stratigraphy from the Miocene Reef Complexes of Mediterranean Regions. Concepts in Sedimentology and Paleontology. Society for Sedimentary Geology, Tulsa, pp. 3–54.

Faranda, C., Cipollari, P., Cosentino, D., Gliozzi, E., Pipponzi, G., 2007. Late Miocene ostracod assemblages from eastern Mediterranean coral-reef complexes (central Crete, Greece). Revue de Micropaléontologie 1–22.

Fassoulas, C., 2001. The tectonic development of a Neogene basin at the leading edge of the active European margin: the Heraklion basin, Crete, Greece. Journal of Geodynamics 31, 49–70.

Fauquette, S., Suc, J.-P., Bertini, A., Popescu, S.-M., Warny, S., Taoufiq, N.B., Villa, M.-J.P., Chikhi, H., Feddi, N., Subally, D., Clauzon, G., Ferrier, J., 2006. How much did climate

force the Messinian salinity crisis? Quantified climatic conditions from pollen records in the Mediterranean region. Palaeogeography, Palaeoclimatology, Palaeoecology 238, 281–301.
Felis, T., Pätzold, J., Loya, Y., Fine, M., Nawar, A.H., Wefer, G., 2000. A coral oxygen isotope record from the northern Red Sea documenting NAO, ENSO, and North Pacific teleconnections on Middle East climate variability since the year 1750. Paleoceanography 15, 679–694.
Felis, T., Lohmann, G., Kuhnert, H., Lorenz, S.J., Scholz, D., Pätzold, J., Al-Rousan, S.A., Al-Moghrabi, S.M., 2004. Increased seasonality in Middle East temperatures during the last interglacial period. Nature 429, 164–168.
Flecker, R., Ellam, R.M., 1999. Distinguishing climatic and tectonic signals in the sedimentary successions of marginal basins using Sr isotopes: an example from the Messinian salinity crisis, Eastern Mediterranean. Journal of the Geological Society 156 (4), 847–854.
Flecker, R., Ellam, R.M., 2006. Identifying Late Miocene episodes of connection and isolation in the Mediterranean–Paratethyan realm using Sr isotopes. Sedimentary Geology 188–189, 189–203.
Flecker, R., De Villiers, S., Ellam, R.M., 2002. Modelling the effect of evaporation on the salinity — $^{87}Sr/^{86}Sr$ relationship in modern and ancient marginal-marine systems: the Mediterranean Messinian Salinity Crisis. Earth and Planetary Science Letters 203, 221–233.
Frydas, D., Keupp, H., Bellas, S., 2008. Stratigraphical investigations based on calcareous and siliceous phytoplankton assemblages from the Upper Cenozoic deposits of Messara Basin, Crete, Greece. Zeitschrift der Deutschen Gesellschaft für Geowissenschaften 159 (3), 415–437.
Gagan, M.K., Ayliffe, L.K., Beck, J.W., Cole, J.E., Druffel, E.R.M., Dunbar, R.B., Schrag, D.P., 2000. New views of tropical paleoclimates from corals. Quaternary Science Reviews 19, 45–64.
Ghil, M., Allen, M.R., Dettinger, M.D., Ide, K., Kondrashov, D., Mann, M.E., Robertson, A.W., Saunders, A., Tian, Y., Varadi, F., Yiou, P., 2002. Advanced spectral methods for climatic time series. Reviews of Geophysics 40. doi:10.1029/2001RG000092.
Hardenbol, J., Thierry, J., Farley, M.B., Jacquin, T., de Graciansky, P.-C., Vail, P.R., 1998. Mesozoic and Cenozoic sequence stratigraphic framework of European Basins. In: de Graciansky, P.-C., Hardenbol, J., Thierry, J., Vail, P.R. (Eds.), Mesozoic and Cenozoic Sequence Stratigraphy of European Basins. SEPM Special Publication. Society for Sedimentary Geology, Tulsa, pp. 3–14.
Hilgen, F.J., Krijgsman, W., Langereis, C.G., Lourens, L.J., Santarelli, A., Zachariasse, W.J., 1995. Extending the astronomical (polarity) time scale into the Miocene. Earth and Planetary Science Letters 136 (3–4), 495–510.
Hilgen, F.J., Krijgsman, W., Wijbrans, J.R., 1997. Direct comparison of astronomical and $^{40}Ar/^{39}Ar$ ages of ash beds: potential implications for the age of mineral dating standards. Geophysical Research Letters 24 (16), 2043–2046.
Hodell, D.A., Mueller, P.A., McKenzie, J.A., Mead, G.A., 1989. Strontium isotope stratigraphy and geochemistry of the late Neogene ocean. Earth and Planetary Science Letters 92, 165–178.
Horwitz, E.P., Chiarizia, R., Dietz, M.L., 1992. A novel strontium-selective extraction chromatographic resin. Solvent Extraction and Ion Exchange 10 (2), 313–336.
Hsü, K.J., Montadert, L., Bernoulli, D., Cita, M.B., Ericson, A., Garrison, R.E., Kidd, R.B., et al., 1977. History of the Mediterranean salinity crisis. Nature 267, 399–403.
Kirby, M.X., 2001. Differences in growth rate and environment between Tertiary and Quaternary *Crassostrea* oysters. Paleobiology 27 (1), 84–103.
Kleypas, J.A., McManus, J.W., Menez, L.A.B., 1999. Environmental limits to coral reef development. Where do we draw the line? American Zoologist 39, (146–159).
Kouwenhoven, T.J., Seidenkrantz, M.-S., van der Zwaan, G.J., 1999. Deep-water changes: the near-synchronous disappearance of a group of benthic foramnifera from the Late Miocene Mediterranean. Palaeogeography, Palaeoclimatology, Palaeoecology 152, 259–281.
Krijgsman, W., Hilgen, F.J., Langereis, C.G., Santarelli, A., Zachariasse, W.J., 1995. Late Miocene magnetostratigraphy, biostratigraphy and cyclostratigraphy in the Mediterranean. Earth and Planetary Science Letters 136 (3–4), 475–494.
Krijgsman, W., Hilgen, F.J., Raffi, I., Sierro, F.J., Wilson, D.S., 1999. Chronology, causes and progression of the Messinian salinity crisis. Nature 400, 652–655.
Kroeger, K.F., Reuter, M., Brachert, T.C., 2006. Palaeoenvironmental reconstruction based on non-geniculate coralline red algal assemblages in Miocene limestone of central Crete. Facies 52 (3), 381–409.
Kurths, J., Spiering, C., Müller-Stoll, M., Striegler, U., 1993. Search for periodicities in Miocene tree ring widths. Terra Nova 5, 359–363.
Lear, C.H., Elderfield, H., Wilson, P.A., 2003. A Cenozoic seawater Sr/Ca record from benthic foraminiferal calcite and its application in determining global weathering fluxes. Earth and Planetary Science Letters 208, 69–84.
Lough, J.M., Barnes, D.J., 2000. Environmental controls on growth of the massive coral *Porites*. Journal of Experimental Marine Biology and Ecology 245, 225–243.
Martín, J.M., Braga, J.C., 1994. Messinian events in the Sorbas basin in southeastern Spain and their implications in the recent history of the Mediterranean. Sedimentary Geology 90, 257–268.
McArthur, J.M., Howarth, R.J., Bailey, T.R., 2001. Strontium Isotope Stratigraphy: LOWESS Version 3. Best-fit line to the marine Sr-isotope curve for 0 to 509 Ma and accompanying look-up table for deriving numerical age. Journal of Geology 109, 155–170.
Mertz-Kraus, R., Brachert, T.C., Galer, S.J.G., Stoll, B., Jochum, K.P., 2007. Seasonal element and Sr isotope ratio variations in Late Miocene corals from Crete, Eastern Mediterranean. Geochimica et Cosmochimica Acta 71 (15, Supplement 1), A656.
Mertz-Kraus, R., Brachert, T.C., Reuter, M., 2008. *Tarbellastraea* (Scleractinia): a new stable isotope archive for Late Miocene paleoenvironments in the Mediterranean. Palaeogeography, Palaeoclimatology, Palaeoecology 257 (3), 294–307.
Meulenkamp, J.E., Sissingh, W., 2003. Tertiary palaeogeography and tectonostratigraphic evolution of the Northern and Southern Peri-Tethys platforms and the intermediate domains of the African–Eurasian convergent plate boundary zone. Palaeogeography, Palaeoclimatology, Palaeoecology 196 (1–2), 209–228.
Meulenkamp, J.E., Dermitzakis, M., Georgiadou-Dikeoulia, E., Jonkers, H.A., Böger, H., 1979. Field Guide to the Neogene of Crete. University of Athens, Athens.
Miller, K.G., Kominz, M.A., Browning, J.V., Wright, J.D., Mountain, G.S., Katz, M.E., Sugarman, P.J., Cramer, B.S., Christie-Blick, N., Pekar, S.F., 2005. The Phanerozoic record of global sea-level change. Science 310 (5752), 1293–1298.
Paillard, D., Labeyrie, L., Yiou, P., 1996. Macintosh program performs time-series analysis. EOS Transactions of the American Geophysical Union 77 (39), 379.
Perez-Folgado, M., Sierro, F.J., Barcena, M.A., Flores, J.A., Vazquez, A., Utrilla, R., Hilgen, F.J., Krijgsman, W., Filippelli, G.M., 2003. Western versus eastern Mediterranean paleoceanographic response to astronomical forcing: a high-resolution microplankton study of precession-controlled sedimentary cycles during the Messinian. Palaeogeography, Palaeoclimatology, Palaeoecology 190, 317–334.
Pierre, C., 1999. The oxygen and carbon isotope distribution in the Mediterranean water masses. Marine Geology 153, 41–55.
Pomar, L., 1991. Reef geometries, erosion surfaces and high-frequency sea-level changes, upper Miocene reef complex, Mallorca, Spain. Sedimentology 38, 243–270.
Poulos, S.E., Drakopoulos, P.G., Collins, M.B., 1997. Seasonal variability in sea surface oceanographic conditions in the Aegean Sea (Eastern Mediterranean): an overview. Journal of Marine Systems 13 (1–4), 225–244.
Reuter, M., Brachert, T.C., 2007. Freshwater discharge and sediment dispersal — control on growth, ecological structure and geometry of Late Miocene shallow-water coral ecosystems (early Tortonian, Crete/Greece). Palaeogeography, Palaeoclimatology, Palaeoecology 255, 308–328.
Reuter, M., Brachert, T.C., Kroeger, K.F., 2005. Diagenesis of growth bands in fossil scleractinian corals: identification and modes of preservation. Facies 51, 155–168.
Reuter, M., Brachert, T.C., Kroeger, K.F., 2006. Shallow-marine carbonates of the tropical — temperate transition zone: effects of hinterland climate and basin physiography (Late Miocene, Crete/Greece). In: Pedley, H.M., Carannante, S. (Eds.), Cool-Water Carbonates. Geological Society of London, Special Publication. Geological Society of London, London, pp. 157–178.
Rohling, E.J., Abu-Zied, R.H., Casford, J.S.L., Hayes, A., Hoogakker, B.A.A., 2008. The Mediterranean Sea: present and past. In: Woodward, J.C. (Ed.), The Physical Geography of the Mediterranean. Oxford University Press, Oxford, UK.
Rosen, B.R., 1999. Paleoclimatic implications of the energy hypothesis from Neogene corals of the Mediterranean region. In: Agusti, J., Rook, L., Andrews, P. (Eds.), The Evolution of Neogene Terrestrial Ecosystems in Europe. Cambridge University Press, pp. 309–327.
Rosenfeld, M., Yam, R., Shemesh, A., Loya, Y., 2003. Implication of water depth on stable isotope composition and skeletal density patterns in a *Porites lutea* colony: results from a long-term translocation experiment. Coral Reefs 22 (4), 337–345.
Rouchy, J.M., Caruso, A., 2006. The Messinian salinity crisis in the Mediterranean basin: a reassessment of the data and an integrated scenario. Sedimentary Geology 188–189, 35–67.
Roulier, L.M., Quinn, T.M., 1995. Seasonal- to decadal-scale climatic variability in southwest Florida during the middle Pliocene: inferences from a coralline stable isotope record. Paleoceanography 10 (3), 429–443.
Sachse, M., Mohr, B.A.R., 1996. Eine obermiozäne Makro- und Mikroflora aus Südkreta (Griechenland), und deren paläoklimatische Interpretation.— Vorläufige Betrachtungen. Neues Jahrbuch für Geologie und Paläontologie. Abhandlungen 200 (1/2), 149–182.
Sánchez-Almazo, I.M., Braga, J.C., Dinarès-Turell, J., Martín, J.M., 2007. Palaeoceanographic controls on reef deposition: the Messinian Cariatiz reef (Sorbas Basin, Almaría, SE Spain). Sedimentology 54, 637–660.
Santarelli, A., Brinkhuis, H., Hilgen, F.J., Lourens, L.J., Versteegh, G.J.M., Visscher, H., 1998. Orbital signatures in a Late Miocene dinoflagellate record from Crete (Greece). Marine Micropaleontology 33, 273–297.
Schenau, S.J., Antonarakou, A., Hilgen, F.J., Lourens, L.J., Nijenhuis, I.A., van der Weijden, C.H., Zachariasse, W.J., 1999. Organic-rich layers in the Metochia section (Gavdos, Greece): evidence for a single mechanism of sapropel formation during the last 10My. Marine Geology 153, 117–135.
Sierro, F.J., Flores, J.A., Francés, G., Vazquez, A., Utrilla, R., Zamarreno, I., Erlenkeuser, H., Barcena, M.A., 2003. Orbitally controlled oscillations in planktic communities and cyclic changes in western Mediterranean hydrography during the Messinian. Palaeogeography, Palaeoclimatology, Palaeoecology 190, 289–316.
Slowey, N.C., Crowley, T.J., 1995. Interdecadal variability of Northern Hemisphere circulation recorded by Gulf of Mexico corals. Geophysical Research Letters 22 (17), 2345–2348.
Sprovieri, M., Barbieri, M., Bellanca, A., Neri, R., 2003. Astronomical tuning of the Tortonian $^{87}Sr/^{86}Sr$ curve in the Mediterranean basin. Terra Nova 15, 29–35.
Suc, J.P., 1984. Origin and evolution of the Mediterranean vegetation and climate in Europe. Nature 307, 429–432.
Suc, J.-P., Popescu, S.-M., 2005. Pollen Records and Climatic Cycles in the North Mediterranean Region Since 2.7 Ma. Special Publications, vol. 247(1). Geological Society, London, pp. 147–158.
ten Veen, J.H., Postma, G., 1999. Neogene tectonics and basin fill patterns in the Hellenic outer-arc (Crete, Greece). Basin Research 11 (3), 223–242.
Thomson, D.J., 1982. Spectrum estimation and harmonic analysis. Proceedings of IEEE 70, 1055–1096.
Tzedakis, P.C., 2007. Seven ambiguities in the Mediterranean palaeoenvironmental narrative. Quaternary Science Reviews 26 (17–18), 2042–2066.
Veron, J.E.N., Minchin, P.R., 1992. Correlations between sea surface temperature, circulation patterns and the distribution of hermatypic corals of Japan. Continental Shelf Research 12 (7), 835–857.
Weber, J.N., Woodhead, P.M.J., 1972. Temperature dependence of oxygen-18 concentration in reef coral carbonates. Journal of Geophysical Research 77, 463–473.

Westerhold, T., Bickert, T., Rohl, U., 2005. Middle to late Miocene oxygen isotope stratigraphy of ODP site 1085 (SE Atlantic): new constrains on Miocene climate variability and sea-level fluctuations. Palaeogeography, Palaeoclimatology, Palaeoecology 217 (3–4), 205–222.

Wijmstra, T.A., Young, R., Witte, H.J.L., 1990. An evaluation of the climatic conditions during the Late Quaternary in northern Greece by means of multivariate analysis of palynological data and comparison with recent phytophysiological and climatic data. Geologie en Mijnbouw 69, 243–251.

Zachos, J., Pagani, M., Sloan, L., Thomas, E., Billups, K., 2001. Trends, rhythms, and aberrations in global climate 65 Ma to present. Science 292, 686–693.

Zidianakis, G., Mohr, B., Fassoulas, C., 2004. The Late-Miocene flora of Vrysses, Western Crete — a contribution to the climate and vegetation history. 5th International Symposium on Eastern Mediterranean Geology, Thessaloniki, Greece, pp. 515–518.